

Absolute inelastic Differential Electron Scattering Sections for Te, Xe, N₂
and CO at Near Threshold Impact Energies for 90° Scattering Angle

R. McClain* and S. Trappan

Jet Propulsion Laboratory
California Institute of Technology
Pasadena, CA, 91109, USA

*National Research Council Resident Research Associate

U. S. G. S. # 34.80.CG5

†Main Addresses:

R. McClain: ANCIER@SCN ¶ NASA.GOV

S. Trappan: SANNDOIR@SCN1.JPL.NASA.GOV

Introduction

There is a great deal of need for accurate differential cross sections (DCSS) associated with electron impact excitation of various atomic and molecular species. These cross sections are needed for modeling of various plasma systems (ranging from lasers and material processing plasmas to planetary and astrophysical plasmas) and for guiding development of theoretical and computational schemes. The need is especially acute in the low, near-threshold impact energy region where, due to experimental difficulties, the available data base is very scanty. The error limits are large, and computational methods are not reliable (except in the very near threshold impact energy region).

The situation concerning the experimental difficulties associated with low-energy DCSS measurements in conventional electron beam/molecular beam scattering experiments has been detailed recently by Trajman and Mc Comkey (1994). Here we refer to beam-beam scattering measurements, where electrostatic (possibly in combination with magnetostatic) methods are utilized for handling and energy selecting the electron beam in the electron gun and detector, as conventional measurements. The major practical problem in this approach relates to the dependence of the response function of the electron detector on the residual energy of the scattered electrons. This function can be calibrated at small residual energies or made constant with respect to residual energy at higher impact energies, in principle, but many practical difficulties exist. Such a calibration is based on the isotropic energy and angle dependence of electrons resulting from near threshold ionization of Fe (Pichou et al., 1978; Baunger et al., 1990, 1991) but the method is not applicable at residual energies larger than a few eV. An additional problem associated with this

method (as well as with a similar method described by Nickel et al., 1989) is that the electron gun has to be retuned when one goes from the calibration stage to the measurement stage and this can have an effect on the overall instrument response function.

To avoid these problems LeClain et al. (1996) introduced a time-of-flight (TOF) approach for determining absolute inelastic DCSs at fixed impact energies (E_0) and scattering angles (θ). In the present paper we describe the application of this TOF method to inelastic DCS measurements in He, Xe, N₂, and CO at 0–90° and E_0 ranging from a few tenths of an eV to about 15 eV above threshold. These DCSs can serve as secondary standards for normalizing the angular distributions (representing relative DCSs) measured by conventional electrostatic electron-energy-loss spectrometers for the same excitation at a given impact energy as well as other relative inelastic DCSs associated with nearby energy-loss features. The criteria for a nearby energy-loss feature is that the instrument response function can be considered to be the same for it as for the standard feature. Electrostatic spectrometers have better energy resolution than the TOF method. One can, therefore, derive individual DCSs for unresolved excitations of the TOF method by utilizing the relative scattering intensities obtained in the conventional measurements in combination with the absolute DCS obtained for the unresolved excitations of the TOF measurement. This procedure was used in the case of Xe by Khakoo et al. (1996a and b) and will be demonstrated for the case of N₂ here.

2. Experimental Apparatus and Procedures

A detailed description of the TOF apparatus and its operation has been published earlier (Le Clair et al., 1996) but we will present a brief summary here. Essentially, the apparatus consists of a mutually orthogonal electron beam, gas beam, and drift tube. These items are placed in a magnetically shielded vacuum chamber (residual magnetic field is less than 2 mG).

We used a simple electron gun which is capable of producing a highly collimated electron beam of up to 220 nA (in the d.c. mode) from a few to several hundred eV impact energies. When operated in the pulsed mode, the gun could typically produce gaussian shaped pulses with a width of several ns, depending on the electron impact energy (E_0). We calibrated E_0 by observing the onset of metastable production for each target gas using a neutral metastable detector. There were no energy dispersing elements in the electron gun, so the width of the energy distribution (δE) was about 0.6 eV, typical of thermoionic sources.

The drift tube was constructed out of sheet molybdenum. Two apertures at the tube entrance were used to define the view cone which had an apex of 6° . The end of the drift tube was terminated with a grid, followed by post-acceleration of 450 V onto a 40 mm diameter multi-channel detector array. This array was followed by two identical arrays to further amplify the signal. The field free drift distance for scattered electrons was 21.6 cm, giving an electron time of flight of $t = 364/\sqrt{E_s}$, where E_s is the residual energy of the scattered electron in eV. The time spent in post-acceleration region was practically constant for the range of residual energies observed with our apparatus.

TOF spectra were acquired by using a standard time-to-amplitude converter and pulse height analyzer operating under the control of a personal computer. Using a pulse rate of 100 KHz, the data acquisition time ranged from 1/2 to 24 hrs in order to obtain intensities of 10,000 counts or more for the features of interest. Intensities were determined from TOF spectra by integrating the number of electron counts for the features of interest after the background was subtracted. As the impact energy increased, inelastic features which overlapped were unfolded by a computer program which could fit multiple gaussians to a specific feature. When two features overlapped by more than their full-widths at half maximum, the unfolding could no longer be applied with much confidence.

A TOF spectrum of He is shown in figure (a). From left to right, the features are due to electrons which have scattered elastically, excited the $n = 3$ manifold of states (double peak), the $n = 3$ manifold, and the long tail arises from the higher manifolds and secondary electrons due to ionization. The first peak in the $n = 2$ manifold structure is due the 2^3S state; it is just barely resolved from second peak, which arises from the 2^1S , 2^3P , and 2^1P states. To aid the identification of features in the TOF spectra, it is convenient to transform TOF spectra from the time domain to the residual energy domain by a change of variable. That is, $P(T)$ represents a TOF spectrum, then the residual energy E_i $\text{min } P(T_i)$ is given by

$$P(T_i) = P(T) \cdot T^3 \quad (1)$$

We can then plot $P(T_i)$ as a function of energy loss which is given by $\Delta E = E_0 - E_i$. An example is shown in Fig. (b), which is an electron energy loss spectrum of fig. (a). One can see that the T^3

factor in (1) greatly exaggerates the noise at long flight times. The width of a feature (ΔE_{res}) in an energy loss spectrum is given approximately by

$$\Delta E_{\text{res}} \approx \frac{E_{\text{AR}}^{3/2} t_w}{8.44 D} + \delta E, \quad (2)$$

where E_{AR} is the average residual energy associated with the feature, t_w is the width of the electron pulse, and D is the drift distance. It can be seen in Fig. 1 (b) that features with high residual energy (i.e., elastic scattering) will have a large width, while features with low residual energy have a width which approaches the energy spread of the incident electron beam.

Since there are 110 focussing elements in the drift tube, we assume that the ratio (R_i) of the intensity associated with an inelastic feature (I_i) to that of an elastic feature (I_{el}) is equal to their corresponding DCS ratios. That is,

$$R_i(E_0, 0) \equiv \frac{I_i(E_0, 0)}{I_{el}(E_0, 0)} = \frac{DCS_i(E_0, D)}{DCS_{el}(E_0, 0)} \quad (3)$$

We use the subscript i to denote a particular inelastic channel. Hereafter, we will refer to R_i as the scattering intensity ratio for channel i and it is understood to be relative to the elastic channel, unless otherwise stated. The assumption in equation (3) is valid for residual energies of few tenths of an eV or more. Below that range, the very weak magnetic fields and patch electric fields from metal surfaces begin to affect the electron trajectories and we cannot be certain that the drift tube is collecting all of the scattered electrons.

The sources of uncertainty in our ratio measurements have also been explained earlier. They mainly arise from the day to day variations in repeatability (1 to 5%), background contributions by reflections of the electron pulse ($\sim 1\%$), and the uncertainties associated with unfolding overlapping features. The latter, of course, gets worse for higher residual energies (or higher) impact energies for the same energy loss process, and is the primary limiting factor for measurements with the present instrument. The errors associated with the inelastic DCS values include, in addition to the above errors, the errors associated with the elastic DCSs (added in quadrature).

3 Results and Discussion

Measurements were carried out for two atomic (He and Xe) and two molecular (N₂ and CO) species. The results will be presented for each species separately and compared to other available experimental and theoretical results.

3.1 Helium

The scattering intensity ratios for the $n=2$ manifold with excitation of the unresolved $n=2$ manifold (2³S, 2¹S, 2³P, and 2¹P) [R_{*n*,*l*}(90)] were measured at $\theta_0 = 22.2, 24.0, 26.0, 28.4$ and 30.0 eV utilizing the TOF spectrometer. These impact energies were selected to avoid strong resonances which appear in the $n=2$ excitation and elastic channels in the near-threshold region as indicated by the

work of Pichou et al. (1976), Joyce et al. (1976), Brunt et al. (1977), Phillips and Wong (1981), and Allan (1997). A typical TOF spectrum and its corresponding energy loss spectrum at $E_0 = 26.0$ eV is shown in Figs. 1a and 1b, respectively. The measured ratios are given in Table 1.

Using (3), the measured intensity ratios were combined with the elastic DCS values [$DCS_{\text{elas}}(90)$] reported by Register et al. (1980) to yield the 90° DCS values for excitation of the combined $n=2$ manifold [$DCS_{n=2}(90)$] at each impact energy. The inelastic DCS values derived by this approach are more accurate than those obtained so far from conventional energy-loss spectra and could be used as secondary standards for normalization of relative angular distributions of $n=2$ excitation cross sections obtained from conventional energy-loss spectra. The $DCS_{n=2}(90)$ values derived from the present TOF measurements and the associated error limits are also summarized in Table I. This table also contains $DCS_{n=2}(90)$ values obtained from conventional energy-loss spectra measured by Hall et al. (1973), Allan (1997), Cartwright et al. (1992), and Trajmar et al. (1992) as well as theoretical results from the 2P -state R-matrix calculations of Fong et al. (1995) and the completely converged close coupling, (ccc) calculations of Fursa and Bray (1995). For completeness the elastic DCS values used in the present work and obtained by interpolations from the measurements of Register et al. (1980) are also given in Table I. The procedure for obtaining the error limits for the present results have been described above. For other results, the error limits were taken from the original publications. All $DCS_{n=2}(90)$ results are also shown and compared in Fig. 2.

The $DCS_{n=2}(90)$ values of Allan (1997) seem to converge to the present TOF results at around 24 eV impact energy and are, within (the rather large) error limits, in agreement with the

tit results at $I_0^i = 22.2$ and 23.2 eV. The trend at lower impact energies is, however, opposite for the two measurements. The $i_0 = 29.2$ eV results of Hall et al. (1973) and the $I_0^i = 30$ eV results obtained from the measurements of Cartwright et al. (1992) and Trajmar et al. (1992) will be compared with the present TOF result within the corresponding error limits. The trend in the TOF data with increasing impact energy is reconcilable with the $i_0 = 39.2$ and 48.2 eV results of Hall et al. (1993) and the $i_0 = 50$ eV results obtained from the measurements of Cartwright et al. (1992) and Trajmar et al. (1992). The *ab initio* calculations of Pura and Bray (1995) show excellent agreement with the present TOF values for $R_{n,2}(90)$, except at the very lowest impact energies. It should be noted, however, that both the $DCS_{n,2}(90)$ and $DCS_{class}(90)$ values obtained by Trajmar et al. (1992) are larger than those derived from the present TOF measurements and the elastic measurements of Register et al. (1980), respectively. The 29-state R-matrix yielded $DCS_{n,2}(90)$ values which are in agreement with other results at $I_0^i = 31.2$ eV but about 50% larger than other results at $I_0^i = 28.4$ eV. This is somewhat surprising because one would expect more reliable results at the lower impact energy

=, the present results represent considerable improvements in establishing the proper value of $DCS_{n,2}(90^\circ)$ in the \Rightarrow to 30 eV impact energy range and could be utilized to normalize relative $DCS_{n,2}(0)$ angular distributions and individual DCS's associated with the individual $2^3S, 2^1S, 2^3P,$ and 2^1P excitations once their relative values have been established from high resolution energy-loss spectra. Decomposition of $DCS_{n,2}(90)$ into individual excitation cross sections can be achieved by utilizing high-resolution energy-loss spectra, obtained by conventional electrostatic electron-impact spectrometers, assuming that the instrument response function remains constant over the energy-loss region \Rightarrow to the $n=2$ manifold excitations. These spectra are not presently available at

the specific impact energies (and 90° angle) considered here.

3.2 Xenon

TOF measurements for Xe were carried out at $\Theta = 90^\circ$ for impact energies ranging from 9 to 20 eV. A typical energy loss spectrum at $E_0 = 12.0$ eV is shown in Fig. 3. The peak in the 8.3 to 8.5 eV energy-loss region, designated as Region 1 corresponds to excitation of the lowest two levels of Xe. The feature in the 9.4 to 10.6 eV energy-loss region, designated as Region 11, corresponds to excitation of the next 18 energy levels. From the TOF spectra, it was possible to deduce the scattering intensity ratios for excitation of the combined two lowest levels [$R_{1+2}(90)$] at impact energies of less than 15.0 eV. At impact energies of 15.0 eV and above, we could determine only the scattering intensity ratios for excitation of the combined twenty lowest levels corresponding to twelve features [$R_{1+20}(90)$]. At these impact energies, utilizing a conventional electrostatic energy-loss spectrometer, we determined the relative scattering intensities for excitation of the combined two lowest levels with respect to the combined next eighteen levels. From these two measurements we deduced the $R_{1+2}(90)$ values, which in combination with the $DCS_{\text{clas}}(90^\circ)$ values of Register et al. (1986), yield the $DCS_{1+2}(90)$ values. The level and region designations and excitation energies that we are concerned with are listed in Table 2. A summary of the present cross sections and those available from other experimental and theoretical works are summarized in Table 3 and Fig. 4.

Comparison of the present results with other available data can be briefly summarized as

follows. Nishimura et al. (1985, 1994) and Filipovic et al. (1988) obtained $DCS_{1,2}(90^\circ)$ values based on their measurements of scattering intensity ratios for excitation of these two levels and elastic DCS's (90°) values, Nishimura et al. (1985, 1994) used elastic DCS's (90°) measured in a separate experiment (Nishimura et al., 1987) while Filipovic et al. (1988) used the elastic $1(X'S(90^\circ))$ of Register et al. (1987). Ester anti Kessler (1994) also obtained the $DCS_{1,2}(90^\circ)$ values by an absolute measurement scheme. All these results are given in Table 3 with their error limits. (Nishimura et al. did not specify the error limits.) Theoretical results are available from first order many body (Khakoo et al. 1996), distorted wave (Bartschat and Madison 1987, 1992 a and b, and 1995) and relativistic distorted wave (Zuo et al. 1991, 1992 a and b) calculations. As can be seen from Table 3 and Fig. 4, there are large discrepancies among the experimental results and between experiment and theory. None of the theoretical approaches discussed here are reliable at low impact energies. It would be valuable to carry out calculations in this energy range based on the close coupling method.

The present $1X_{1,2}(90^\circ)$ values represent a significant improvement in the error limits and fills the gap between the threshold and 15 eV impact energy range. They could serve as secondary standards for normalizing inelastic $1DCS(\theta)$ curves. Indeed this was done by Khakoo et al. (1996a) to obtain absolute $1DCS_{1,2}(\theta)$ values at 10, 15 and 20 eV impact energies over the 0° to 135° angular range and with these in turn $DCS(\theta)$ values for excitation of the next 18 states in Xe (Khakoo et al. 1996b).

3.3 Nitrogen

In the case of N_2 , TOF measurements were carried out at $\theta = 90^\circ$ at impact energies ranging from 7.0 eV to 20.0 eV. The present TOF method can not resolve individual electronic transitions but only regions of the energy-loss spectra which correspond to several overlapping electronic transitions and their vibrational band structures. These regions and the corresponding electronic states are listed in Table 4 and are shown in a typical energy loss spectrum in Fig. 5. Region I extends from 6.5 to 10.8 eV energy loss and contains seven electronic state excitations ($A^3\Sigma_u^+$, $B^3\Pi_g$, $W^3\Delta_u$, $a^1\Pi_g$, $w^1\Delta_u$, $a'^1\Sigma_u$ and $B'^3\Sigma_u^+$). A second group of excitation features appears in the TOF spectra in the 10.8 to 12.4 eV energy-loss range which we designate as Region II. This feature contains the excitation of the $C^3\Pi_u$, $E^3\Sigma_g^+$ and $a''^1\Sigma_g^+$ states. At 14 eV or higher impact energies, a third feature appears in the 12.4 to 13.5 eV energy-loss region which we designate as Region III. This feature contains the excitations of eight electronic states ($b^1\Pi_u$, $D^3\Sigma_u^+$, $G^3\Pi_u$, $c^1\Pi_u$, $c'^1\Sigma_u^+$, $F^3\Pi_u$, $o^1\Pi_u$ and $b'^1\Sigma_u^+$). Two additional features appear in the TOF spectra at higher impact energies but the relative scattering intensities associated with them can not be meaningfully evaluated. From the TOF spectra we determined the scattering intensity ratios for Regions I, II, and III within error limits of $\pm 5\%$, $\pm 15\%$, and 50% , respectively. These ratios are given in Table 5 and in Fig. 6 at impact energies ranging from 7.5 to 20.0 eV.

Utilizing the 90° elastic DCS results of Shyn and Carignan (1980), we converted the TOF ratios to $DCS_I(90)$ and $DCS_{II}(90)$ values corresponding to excitation of the combined electronic states contained in these regions. In doing these conversions, we look the intensity ratios to be equal

to the corresponding DCS ratios and neglected possible contributions to the elastic feature in the TOF spectra from pure vibrational excitations. These assumptions are well justified based on the TOF method (i.e. Clair et al., 1996) and on the vibrational excitation cross sections as measured by Tanaka et al. (1981). The $DCS_I(90)$ and $DCS_{II}(90)$ values and associated error limits are also listed in Table 5. A comparison of the present $DCS_I(90)$ and $DCS_{II}(90)$ results to those obtained from the measurements of Cartwright et al. (1977) and Brunger and Teubner (1990) is given in Table 6 and shown in Figs. 7 a and b. Those authors determined the relative DCS's associated with excitation of individual levels of N_2 from conventional energy-loss spectra by unfolding techniques similar to ours. Cartwright et al. (1977) normalized the relative inelastic IXX's to the elastic DCS's of Srivastava et al. (1976). Trajmar et al. (1983) renormalized the inelastic IXX'S based on a somewhat improved elastic N_2 DCS set. We used these renormalized inelastic DCS's in the present comparisons. Brunger and Teubner utilized their own elastic DCS's for normalization. The error estimation is somewhat subjective (no rigorous procedure can be applied) and some authors are more conservative than others. The error limits given in Table 6 were obtained from the corresponding papers and they include the estimated errors for the scattering intensity ratio measurement as well as the errors associated with the elastic DCS's. (The deconvolution errors were not considered here, since we are dealing with the combined inelastic processes in an energy-loss region.) It can be seen from Figs. 7 a and b that the results obtained by various researchers differ substantially and that the error limits are large. The two conventional measurements agree in general within these large error limits but in most cases do not overlap with the TOF results within the combined error limits. Recent measurements by Zobelet al. (1996a) yielded inelastic DCS's at impact energies ranging from 0.1 to 3.7 eV above threshold. These measurements were carried out at constant residual

energies and utilized the He I resonance ionization behavior of He for calibrating the instrument function. It is not feasible to extract $\text{DCS}_i(90)$ and $\text{DCS}_{ii}(90)$ values from these experiments (Franck-Condon factors may not apply, there are difficulties associated with generating all individual electronic state excitation cross sections at fixed impact energies from the fixed residual energy data, etc.).

In order to obtain absolute differential cross sections for excitation of individual electronic and vibrational levels at 90° , based on TOF normalization, one needs conventional energy-loss spectra with sufficient resolution to yield relative scattering intensities for these individual excitations. These relative intensities can then be combined with the absolute DCS values obtained by the TOF method for the corresponding energy-loss region. To demonstrate this procedure, we produced conventional energy-loss spectra at a few impact energies at 90° scattering angle (e.g. Fig. 8) and deduced absolute DCS's for excitation of the $A^3\Sigma_u^+$ and $C^3\Pi_u$ states of N_2 . Important comparisons and checks can then be made to data obtained by conventional normalization methods including those of Zobel et al. (1996a).

For the $A^3\Sigma_u^+$ state excitation, DCS (90) values summed over all vibrational levels are available from Cartwright et al. (1977) / Trajmar et al. (1984), and Brunger and Teubner (1990). In these works the validity of the Born-Oppenheimer adiabatic nuclear separation principle was assumed and Franck-Condon factors were used in the unfolding of the energy-loss spectra. We can, therefore, generate DCS's for individual vibrational band excitations in these two cases. Zobel et al. (1996a) produced energy-loss spectra with constant residual energies (corresponding to different

impact energies for each energy-loss value). Since the measurements were carried out at many residual energies, cross sections at fixed impact energies can be extracted from their measurements. However, their measurements were carried out at near threshold impact energies and one cannot assume the applicability of Franck-Condon factors in this region. They reported IX's for excitation of the $A^3\Sigma_u^+$ ($v = 4,5,6$) and $A^3\Sigma_u^+$ ($v = 6$) levels.

Energy loss features up to $v = 6$ for the $A^3\Sigma_u^+$ state are not overlapped by other transitions in the conventional energy-loss spectra and are clearly resolved. Therefore, the uncertainties associated with the unfolding procedure are eliminated. The DCS's for excitation of the $v = 6$ and the combined $v = 4,5,6$ levels determined in the present work are compared with those reported by Zobel et al., and obtained from the results of Brunger and Teubner and Cartwright et al. / Trajmar et al. in Figs. 9 a and b and summarized in Table 7. The present results are consistent with and complement those of Zobel et al. The values derived from the data of Cartwright et al. / Trajmar et al. are in agreement with the present results within the rather large error limits while those of Brunger and Teubner are not.

Results obtained for the $C^3\Pi_u$ state excitations, with similar procedures as described above for the $A^3\Sigma_u^+$ state, are summarized in Table 8 and compared with each other in Figs 10 for excitation of the combined $v = (0, 1, \text{ and } 2)$ levels. The various results are consistent within the rather large error limits except the 15 and 17.5 eV results of Brunger and Teubner. (In this case the conversion of the DCS (90) values obtained by Zobel et al. for $v = 0,1,2$ can be confidently converted to those for all v since the summed Franck-Condon factors for $v = 0,1,2$ is 0.96).

3.4 Carbon Monoxide

For (X), we carried out TOF measurements at 90° angle for impact energies ranging from 6.5 to 15.0 eV. Typical energy-loss spectra are shown in Fig. 11. The first feature corresponds to excitation of the $a^3\Pi$ state (in the 6.8 to 7.3 eV energy-loss region, designated as Region I). The second feature, which appears noticeably above 10 eV impact energies, is dominated by excitation of the $A^1\Pi$ level but minor contributions from the $a^3\Sigma^+$, d^3A , $c^3\Sigma^-$ and $1^1\Sigma^-$ excitations are also present. This feature extends from about 7.6 eV to 10.0 eV energy loss and is designated as Region II. Region I is clearly separated from Region II at $E_0 < 10.0$ eV. At higher energies these regions overlap and unfolding is required to determine scattering intensities for individual regions. From the TOF spectra, we determined the scattering intensities ratios associated with Regions I and II (R_I and R_{II} , respectively). Utilizing the elastic DCS values measured by Gibson et al. (1995), and equation (3), we obtained DCS's for excitation of the $a^3\Pi$ and $A^1\Pi$ states. Some of these results concerning R_I and DCS's for excitation of the $a^3\Pi$ state have been presented in our paper describing the TOF method (LeClair et al., 1996). All the ratio and DCS values obtained from the present measurements, as well as from other measurements and theories, are summarized in Tables 9 and 10 and comparisons are made in Figures 12 and 13.

The results concerning the excitation of the $a^3\Pi$ electronic state are presented and compared with other available data in Table 9 and Fig. 12. Experimental results are available for comparison with the present results from Middleton et al. (1993) and Zobel et al. (1996 b). Although Zobel et al. measured the cross sections associated with excitation of the lowest six vibrational levels of the

a $^3\Pi$ state, their results can be considered to be equivalent to those corresponding to excitation of all vibrational levels since excitation of the lowest six vibrational levels represent 99.2% of the total excitation based on Franck-Condon factors (Cartwright, 1972). Theoretical results are available from Sun et al. (1992) based on Schwinger multichannel variational calculations. Excellent agreement prevails for all experimental data but the theoretical values are too large at $1 \text{ e}_0 > 10 \text{ eV}$.

Results concerning excitation of the combined six electronic states involved in feature 11 in the TOF spectra are summarized in Table 10 and Fig. 13. Results for excitation of the A $^1\Pi$ electronic state alone are also given for comparison. The 90° DCS values obtained for Region 11 and for excitation of the A $^1\Pi$ state in the various investigations are in agreement with the combined error bars.

4. Summary and Conclusions

It has been demonstrated that electron TOF spectroscopy can be utilized for obtaining absolute DCS's for excitation processes at low electron impact energies. Although the energy resolution of our TOF apparatus was not sufficient to resolve individual electronic transitions, it can be combined with conventional energy-loss spectroscopy (which is capable of higher energy resolution) to extract absolute DCS's for many more individual excitations. The TOF method is applicable in the impact energy region from threshold to about 10 to 20 eV above threshold depending on the structure of the energy-loss spectrum. This is a very important region since

methods based on near threshold ionization of 1 Ic (like Zobel et al., 1996 b) are limited to within 3 eV above threshold and the troublesome effect of residual energy dependence of the instrument response function for conventional electron impact spectrometers diminishes to negligible limits only at impact energies of about 20 eV above threshold. The TOF method thus fills the gap for absolute DCS measurements.

The TOF calibration method was demonstrated for 1 Ic, Xe, N₂ and CO. In general, the TOF results are consistent with other available data at the higher and near-threshold impact energies. The available data are rather limited and are associated with large error limits. The TOF approach represents a considerable improvement in the accuracy of the DCS's and is more practical at near threshold impact energies than the method of Zobel et al. (1996 b). Further improvements in the energy resolution of our apparatus is desirable. It requires the application of an energy selected initial electron beam (which comes with sacrifice in the signal levels). Such an effort is in progress in our laboratory. There is need for more reliable theoretical results to extend the range of experimental data to wider energy and angular ranges and to guide the deduction of general trends and consistency for the ICS's data base.

5. Acknowledgements

This work was carried out at the Jet Propulsion Laboratory, (California Institute of Technology) and was supported by the National Aeronautics and Space Administration. The authors wish to

express their gratitude to J. C. Gibson, V. Mc Key, and J. Zobel for valuable discussions and for supplying us unpublished results and to M. A. Khakoo for supplying us equipment and material used in our measurements as well as for helpful discussions. One of us (I. R. L.) is grateful to the NRC for being awarded a Resident Research Associateship.

References

Allan M 1992 *J. Phys. B.* 251559

Bartschat K and Madison I D H 1987 *J. Phys. B: At. Mol. Phys.* 205839, 1992a *J. Phys. B: At. Mol. Opt. Phys.* 251361, 1992b *J. Phys. B: At. Mol. Opt. Phys.* 254619, and private communication, 1995

Brunger M J, Buckman S J and Newman D 1990 *Aust. J. Phys.* **43** 665

Brunger M J, Buckman S J, Newman D 1) and Allen D '1' 1991 *J. Phys. B: At. Mol. and Opt. Phys.* 241435

Brunger M J, Teubner P 1990 *Phys. Rev. A* 41 1413

Brunt J N 1), King G C and Read D 1977 *J. Phys. B.* 10433

Carlwright D C 1972, private communication, to be published

Carlwright D C, Chutjian A, Trajmar S and Williams W 1977 *Phys. Rev. A* **16**1013

Carlwright D C, Csanak G, Trajmar S and Register D F 1992 *Phys. Rev. A* 451602

Estler T and Kessler J 1994 *J. Phys. B: At. Mol. Opt. Phys.* 274295

Filipović D, Marinković B, Pejčev V and Vušković I. 1988 *Phys. Rev. A* **37** 356

Fon W C, Jim K P, Berrington K A and Jones '1' G 1995 *J. Phys. B.* **28** i 569

Fursa D V and Bray I 1995, to appear in *Phys. Rev. A*

Gibson J C, Morgan L., Gulley R J, Brunger M J and Buckman S J 1995, to be published, private communication

Hall R 1, Joyez G, Mazeau J, Reinhardt J and Schermann C 1973 *Journal de Physique* **34** 827

Joyez G, Heutz A, Pichon I: and Mazeau J 1976 in *Electron and Photon Interaction with Atoms* Eds. Kleinpoppen H and McDowell M R C, Plenum Publishing Corp, New York 2.9349

Khakoo M A, Trajmar S, LeClair I, R, Kanik I, Csanak G and Fontes C J 1996a *J. Phys. B: At. Mol. Opt. Phys.* (submitted)

Khakoo M A, Trajmar S, Wang S, Kanik I, Aguirre A, Fontes C, Clark R E H and Abdallah J Jr, 1996b *J. Phys. B: At. Mol. Phys.* (submitted)

- LeClair I. R, Trajmar S, Khakoo M A and Nickel J C 1996, to appear in *Rev.Sci.Instr.*
- Middleton A G, Brunger M J and Teubner P J () 1993 *J. Phys. B.* 261743
- Nickel J, Zetner P, Shen G and Trajmar S 1989 *J. Phys.* 11.22730
- Nishimura H, Danjo A and Matsuda T 1985 *Proceedings of the 14th International Conference on the Physics of Electronic and Atomic Collisions (Palo Alto)*, abstracts p. 108, and private communication, 1994
- Nishimura H, Matsuda T and Danjo A 1987 *J. Phys. Japan* 56 70
- Phillips J M and Wong, S F 1981 *Phys. Rev. A* 233324
- Pichou F, Huetz A, Joyez G and Landau M 1978 *J. Phys. /1.: At. Mol. Phys.* 113683
- Pichou F, Huetz A, Joyez G, Landau M and Mazeau J 1976 *J. Phys. B.* 9933
- Register D F, Trajmar S, and Srivastava S K 1980 *Phys. Rev. A* 21 1134
- Register D F, Vušković I, and Trajmar S 1986 *J. Phys. B: At. Mol. Opt. Phys.* **191685**
- Shyn T W and Carignan G R 1980 *Phys. Rev. A* 22923
- Srivastava S K, Chutjian A and Trajmar S 1976 *J. Chem. Phys.* 641340
- Sun Q, Winstead C and McKoy V 1992 *Phys. Rev. A* 466987
- Tanaka H, Yamamoto T and Okada T 1981 *J. Phys. B.* **142081**
- Trajmar S and McConkey J W 1994 *Adv. in At. Mol. and Opt. Phys.* 33 63
- Trajmar S, Register D F, Cartwright D C and Csanak G 1992. *J. Phys. B.* 254889
- Trajmar S, Register D F and Chutjian A 1983 *Physics Reports* 97 219
- Zetner P W, Trajmar S and Kanik I 1996, to be published
- Zobel J 1996a, private communication
- Zobel J, Mayer U, Jung K and Ehrhardt H 1996b, *J. Phys. B.* 29813 and private communication
- Zuo T, McEachran R P and Stauffer A D 1991 *J. Phys. B: At. Mol. Opt. Phys.* 242853, 1992a *J. Phys. B: At. Mol. Opt. Phys.* 253393, and private communication, 1992b

Table 1. Summary of $R_{n=2}(90)$, $DCS_{n=2}(90)$ and $DCS_{elas}(90)$ values and associated error limits for He^(a).

E_0 (eV)	$DCS_{elas}(90)$		$100 \times R_{n=2}(90)$		$DCS_{n=2}(90)$					$DCS_{elas}(90)$	$100 \times R_{n=2}(90)$	
	1	2	2	3	4	5	6	7	8	8	8	
21.5	168 ± 8.4			-	5.87 ± 2.05							
21.8	166 ± 8.3			-	6.12 ± 2.14				8.01	178.4	4.49	
22.0	165 ± 8.3			-	6.43 ± 2.25							
22.2	162 ± 8.1	5.50 ± 0.10	8.91 ± 0.4s	-	6.77 ± 2.37							
23.2	154 ± 7.7	.		-	6.96 ± 2.44				8.39	164.5	5.10	
24.0	147 ± 7.4	4.75 ± 0.10	6.98 ± 0.38	-								
24.2	146 ± 7.3	-		-					7.88	158.0	4.99	
25.8	135 ± 8.1	-		-					7.19	146.5	4.91	
26.0	133 ± 8.0	4.75 ± 0.15	6.32 ± 0.42	-								
27.3	126 ± 7.6			-								
28.4	127 ± 8.8	4.62 ± 0.15	5.59 ± 0.42	-				8.99				
29.2	116 ± 7.0	-		-	5.98 ± 1.20							
30.0	112 ± 7.8	4.61 ± 0.20	5.16 ± 0.42	5.74 ± 1.15			6.78		4.99	115.9	4.31	
31.2	106 ± 6.4	-		-				5.69				
39.2	73 ± 4.4	-		-	3.40 ± 0.54							
40.0	71 ± 4.3			-								
48.2	54 ± 2.7			-	2.80 ± 0.50				2.88	75.3	3.82	
50.0	53 ± 3.2			3.63 ± 0.73								

^(a) All DCS are in 10^{-16} cm²/srunits

1 Register et al. (1980)	- Exp.	6 Cartwright et al. (1992)	- FOMBT
2 Present results	- Exp.	Trajmar et al. (1992)	- FOMBT
3 Cartwright et al. (1992)	- Exp.	7 Fon et al. (1995)	- 29 state cc
4 Allan (1992)	- Exp.	8 Fursa and Bray (1995)	- ccc *
5 Hall et al. (1973)	Exp.		

Table 2. Summary of level and region designations and excitation energies for Xc.

Level No.	Level Designation	Energy (eV) (Moore)	
0	$5p^6 \ ^1S_0$	0.000	
1	$6s \ [^3/2]_2$	8.315	
2	$6s \ [^1/2]_1$	8.437	} Region I
3	$6s \ [^1/2]_0$	9.447	
4	$6s \ [^1/2]_1$	9.570	
5	$6p \ [^1/2]_1$	9.580	} Region II
6	$6p \ [^3/2]_2$	9.686	
7	$6p \ [^3/2]_3$	9.721	
8	$6p \ [^3/2]_1$	9.789	
9	$6p \ [^3/2]_2$	9.821	
10	$5d \ [^1/2]_0$	9.891	
11	$5d \ [^1/2]_1$	9.917	
12	$6p \ [^1/2]_0$	9.934	
13	$5d \ [^7/2]_4$	9.943	
14	$5d \ [^3/2]_2$	9.959	
15	$5d \ [^1/2]_1$	10.039	
16	$5d \ [^3/2]_2$	10.159	
17	$5d \ [^3/2]_3$	10.220	
18	$5d \ [^3/2]_1$	10.401	
19	$7s \ [^1/2]_2$	10.562	
20	$7s \ [^3/2]_1$	10.593/	

Table 3 Summary of inelastic to elastic scattering intensity ratios and DCS values (in 10^{-19} cm² / sr units) for Xe at $\theta = 90^\circ$ and associated error limits.

E_0 (eV)	$R_{i+2}(90)$ TOF	$R_{i+2}(90)^{(a)}$ TOF	$R_{i+2}(90)^{(a)}$ TOF + ES	DCS _{el} (90°) ^(b)	TOF	1	2	DCS _{i+2} (90) 3	4	5	ϵ
9	0.20 ± 0.02	-	-	850 ± 43	17.0 ± 1.9	-	-	-	-	-	-
10	0.27 ± 0.03	0.044 ± 0.002	-	720 ± 36	19.4 ± 2.3	-	-	-	25.7	-	-
11	0.30 ± 0.02	0.117 ± 0.002	-	640 ± 32	19.2 ± 1.3	-	-	-	-	-	-
12	0.32 ± 0.15	0.156 ± 0.012	-	570 ± 29	18.2 ± 1.3	-	-	4.7	-	-	-
13	0.29 ± 0.15	0.182 ± 0.010	-	515 ± 26	14.9 ± 1.0	-	-	-	-	-	-
14	0.28 ± 0.02	0.201 ± 0.008	-	465 ± 23	13.0 ± 1.2	-	-	-	-	-	-
15	-	0.212 ± 0.007	0.027 ± 0.003	420 ± 21	11.3 ± 1.0	1.7 ± 2.4	19.1 ± 4.4	0.8	35.3	28.3	-
16	-	0.217 ± 0.007	-	385 ± 19	-	-	-	-	-	-	-
17	-	0.206 ± 0.003	-	350 ± 18	-	-	-	-	-	-	-
17.5	-	-	-	335 ± 17	-	-	-	3.0	-	-	-
18	-	0.211 ± 0.002	-	320 ± 16	-	-	-	-	-	-	-
19	-	0.210 ± 0.005	-	290 ± 15	-	-	-	-	-	-	-
20	-	0.208 ± 0.005	0.026 ± 0.003	265 ± 16	6.9 ± 0.6	-	11.8 ± 2.2	7.6	18.5	14.5	17.1
25	-	-	-	180 ± 14	-	-	-	5.2	-	-	-
30	-	-	-	133 ± 12	-	4.9 ± 0.6	13.3 ± 2.9	4.3	7.6	2.5	4.1
50	-	-	-	-	-	-	-	-	-	0.64	2.91
80	-	-	-	-	-	0.25 ± 0.03	-	-	0.68	0.43	0.90

Kh

RD

Table 4. Electronic excited states of N₂ observed in TOF spectra.

States	onset (eV)	Regions
A ³ Σ _u ⁺	6.17	
B ³ Π _g	7.35	
W ³ Δ _u	7.36	I
B' ³ Σ _u ⁻	8.16	
a' ¹ Σ _u ⁻	8.40	
a ¹ Π _g	8.55	
w ¹ Δ _u	8.89	v
C' ¹ Π ⁺	1.03	
E' ³ Σ _g ⁺	1.88	II
a'' ¹ Σ _g ⁺ (only v=0)	2.25	
b' ¹ Π ⁺	2.58	
G' ¹ Π ⁺	2.84	
D' ³ Σ _u ⁺	12.81	
c' ¹ Π _u	12.91	III
c' ¹ Σ _u ⁺	12.94	
F ³ Π _u	12.98	
o' ¹ Π _u	13.10	
b' ¹ Σ _u ⁺	13.22	

Table 5. Summary of the present TOF inelastic to elastic intensity ratios for N₂ and DCS's derived from them. The DCS_{elastic} (90) values used are also given.

E ₀ (eV)	I _{00X} R _I (90)	100X R _{II} (90)	I _{00X} R _{III} (90)	DCS _{elas} (90) ^(a)	DCS _I (90) (10 ⁻¹⁸ cm ² / sr)	DCS _{II} (90)
7.5	0.87			57.0	0.50	
8.0	2.42			53.0	1.28	
8.5	4.61			49.0	2.26	
9.0	6.81			45.0	3.06	
9.5	9.95			42.5	4.23	
10.0	13.2			39.0	5.15	
10.5	16.7			37.0	6.18	
11.0	19.0			35.0	6.65	
11.5	19.6			33.0	6.47	
12.0	19.9			31.5	6.27	
12.5	20.1			30.0	6.03	
13.0	20.5	4.02		28.5	5.84	1.15
13.5	21.0	7.54		27.5	5.78	2.07
14.0	22.1	10.2	2.07	26.0	5.75	2.65
14.5	23.3	10.3	2.85	25.0	5.83	2.58
15.0	24.1	9.71	4.35	24.0	5.78	2.33
15.5	25.4	9.41	4.14	23.5	5.97	2.21
16.0	25.9	8.94	4.11	22.6	5.85	2.02
16.5	26.2	8.29	4.70	22.0	5.76	1.82
17.0	26.0	7.96	4.97	21.5	5.59	1.71
17.5	25.7	8.10	5.70	21.0	5.40	1.70
18.0	25.3	8.10	5.8	20.0	5.06	1.62
18.5	25.1	8.56	5.94	19.6	4.92	1.68
19.0	24.4	8.66	5.8	19.2	4.68	1.66
19.5	24.3	8.48	7.04	18.9	4.59	1.60
20.0	24.1	8.00	7.20	18.5	4.46	1.48
Error	± 5%	± 50%	± 50%	± 5%	± 16%	± 21%

^(a)The DCS_{elastic} (90) values were obtained by interpolation from the measured values of Shyn and Carignan (1980).

Table 6. Comparison of present TOF DCS_I (90) and DCS_{II} (90) results for N₂ with those obtained from previous energy-loss spectra measured by conventional electrostatic spectrometers. (All DCS's in 10⁻¹⁸ cm²/sr units.)^(a)

E ₀ (eV)	DCS _I (90)			DCS _{II} (90)		
	1	2	3	1	2	3
10.0	5.09		5.15			
12.5	10.77		6.03			
15.0	10.38	13.70	5.78	3.73	4.90	2.33
17.0	8.09		5.59	2.11		1.41
17.5		11.38	5.40		3.84	1.70
20.0	1.20	1.37	4.46	1.20	1.37	1.48
Errors	± 30%	± 17%	± 16%	± 300/0	± 17%	± 21%

^(a) 1. Cartwright et al. (1977)/ Trajmar et al. (1983)
 2. Brunger and Teubner (1990)
 3. Present TOF

Table 7. Summary of DCS (90) values for excitation of the $A^3\Sigma_u^+$ state in N_2 . The vibrational levels considered for the $A^3\Sigma_u^+$ state are indicated.

E_0 (eV)	DCS (90) in 10^{-18} cm ² / sr units											
	$v = 6$				$v = 4, 5, 6$				all v			
	(1)	(2)	(3)	(4)	(1)	(2)	(3)	(4)	(1)	(2)	(5)	(3)
7.30				0.023				0.080				
7.50				0.051				0.145				
8.50				0.060				0.185			-	
8.6								0.300			1.3	
9.00				0.123				0.374				
9.50				0.183				0.465				
9.80	-			0.1s1				0.466			1.5	
10.0	(0.12)			0.172	(0.29)			0.418	1.48			
10.5				0.132				0.351				
12.0			0.14				0.32	-	-			(1.59)
12.5	(0.12)		-		(0.30)			-	1.51			
14.8			0.13				0.29	-	-			(1.42)
15.0	(0.16)	(0.061)	0.12		(0.39)	(0.15)	0.29	-	1.98	0.74		(1.45)
17.0	(0.16)				(0.38)				1.91			
17.5	-	(0.14)				(0.34)			-	1.70		
20.0	(0.080)	(0.019)			(0.19)	(0.046)			0.97	0.23		-
20.7			0.0s				0.21					(1.03)
Error	$\pm 35\%$	$\pm 200/0$	$\pm 20\%$	$\pm 24\%$	$\pm 35\%$	$\pm 20\%$	$\pm 17\%$	$\pm 24\%$	$\pm 35\%$	$\pm 20\%$		$\pm 17\%$

(1) Cartwright et al. (1977)/ Trajmar et al. (1983)

(2) Brunger-Teubner (1990)

(3) present TOF + EELS

(4) Zobel et al. (1996)

(5) Mazeau et al. (1972)

Values in parenthesis were obtained from original data **using** Franck-Condon factors.

Table 8. Summary of DCS (90) values for excitation of the C $^3\Pi_u$ state in X₂. The vibrational levels considered for the C $^3\Pi_u$ state are indicated.

E_e (eV)	DCS(90) in 10^{-18} cm ² /sr units											
	$v = 0$				$v = 0, 1, 2$				all v			m
	(1)	(2)	(3)	(4)	(1)	(2)	(3)	(4)	(1)	(2)	(3)	
11.60	-	-	-	0.104				0.172				(0.179)
12.0	-	-	0.14	0.162			0.23	0.266			0.24	(0.277)
12.5	0	-	-	0.311				0.473				(0.493)
13.00	-	-	-	0.691				0.884				(0.921)
14.0	-	-	-	1.6	1.6			2.687				(2.799)
14.8	-	-	1.14	1.528			2.13	2.550			2.26	(3.000)
15.0	(1.89)	(2.52)	1.10		(3.32)	(4.42)	2.09	-	3.46	4.60	2.21	-
17.0	(1.01)				(1.78)				1.55	-	-	-
17.5	-	(1.97)			-	(3.46)				3.60		
20.0	(0.55)	(0.59)			(0.96)	(1.04)			1.00	1.08		
20.7	-	0.57			-		1.04				1.09	-
Error	± 35%	± 20%	± 25%	± 24%	± 35%	± 20%	± 22%	± 24%	± 35%	± 20%	± 22%	± 24%

(1) Cartwright et al.(1977)/ Trajmar et al. (1983)

(2) Brunger and Teubner (1990)

(3) Present TOF + EELS

(4) Zobel et al. (1996)

Values in parenthesis were obtained from original data by using Franck-Condon factors.

Table 9. Summary of inelastic to elastic scattering intensity ratios and DCS values for excitation of the a 3,1 state of CO at 90° scattering angle. For completeness the elastic DCS values are also given. All DCS's are in 10⁻¹⁸ cm²/sr units

E ₀ (eV)	1 OoxR ₁ ^(a)	DCS _{el} (90) ^(b)	1	DCS a 3II (90)		
				2	3	4
6.5	4.03 (0.30)	66.0*	2.66	2.5		4.50
7.0	7.58 (0.07)	60.0*	4.55	4.2		6.00
7.5	11.50 (0.20)	54.2	6.24	5.3		
8.0	15.70 (0.20)	49.5*	7.77	6.4		7.41
8.5	18.90 (0.50)	45.8*	8.66	8.0		
9.0	20.90 (0.80)	42.9	8.97	8.9		8.84
9.5	20.40 (0.50)	40.5*	8.24	8.6		
10.0	18.40 (0.70)	38.7*	7.1'2			11.91
10.5	16.20 (0.70)	38.1*	6.17			12.05
11.0	13.90 (0.60)	37.6	5.23			
11.5	11.60 (0.50)	36.7*	4.26			9.98
12.0	10.80 (0.50)	35.5	3.83			
12.5	9.81 (0.50)	34.0*	3.34			8.03
13.0	9.17 (0.50)	32.7	3.00			
13.5	8.79 (0.50)	31.7*	2.79			7.02
14.0	8.37 (0.60)	30.9	2.59			
14.5	8.33 (0.70)	29.7*	2.47			
15.0	8.23 (0.80)	28.6	2.35			5.46
16.5						4.33
18.0						3.91
20.0					1.51	3.26
22.0						
25.0						2.41
30.0					0.83	1.98
40.0					0.36	
50.0					0.23	
Error		± 7%	±100/0	± 24 %	± 250/0	

^(a)The numbers in parenthesis give the error limits (±) for each measurement.

^(b)The elastic 90° DCS values are from Gibson et al. (1995). The values denoted by * have been obtained by interpolation.

- (1) Present TOF
- (2) Zobelet al. (1996)
- (3) Middleton et al. (1993)
- (4) Sun et al. (1992)

Table 10. Summary of inelastic to elastic scattering intensity ratios and DCS values for excitation of the six electronic states contributing to feature II and for the A ¹Π state at $\theta = 90^\circ$ for CO. All DCS's are in $10^{-18} \text{ cm}^2/\text{sr units}$.

E_0 (eV)	I Oxx R _{II} ^(a) (1)	DCS _{el} (90) ^(b)	DCS _{II} (90)			DCS A ¹ Π(90)		
			(1)	(3)	(4) ^(d)	(2)	(3)	(4)
8.25						0.07		
8.50						0.17		
9.0						0.51		
9.5	3.8 (0.6)	40.5 ^{**}	1.54 ^(c)			0.92		
10.0	6.6 (0.6)	38.7*	2.55		2.3	1.51		1.49
10.5	8.3 (0.7)	38.1*	3.16			1.71		
11.0	11.0 (0.9)	37.6	4.14			1.98		
11.5	13.7(1.1)	36.7*	5.03			2.55		
11.75						2.7%		
12.0	16.3 (1.3)	35.5	5.79					
12.5	19.5 (1.6)	34.0*	6.63		5.1			2.30
13.0	22.2 (2.2)	32.7	7.26					
13.5	25.2 (2.5)	31.7*	7.99					
14.0	29.6 (3.0)	30.9	9.15					
14.5	31.3 (3.1)	29.7*	9.30					
15.0	34.0 (3.4)	28.6	9.72		7.7			3.55
20.0				2.26			1.66	
30.0				2.34			1.73	
40.0				1.12			0.80	
50.0				0.85			0.58	
Error %		± 7	± 12	± 25	± 16	± 24	± 25	± 16

^(a) The numbers in parenthesis give the error limits (±) for each data point.

^(b) The elastic DCS(90) values are from Gibson et al. (1995). The values denoted by * have been obtained by interpolation.

^(c) The error limits for this data point are ±17%.

^(d) Contributions from the e³Σ⁻ and f¹Σ⁻ excitations at all E₀ and in addition from the d 3_g excitation at 10 eV were neglected. At E₀ = 10 eV Franck-Condon factors were used to obtain 1 DCS's for all vibrational levels of the final state from results obtained for a few specific vibrational levels.

(1) Present TOF

(2) Zobel et al. (1996 b)

(3) Middleton et al. (1993)

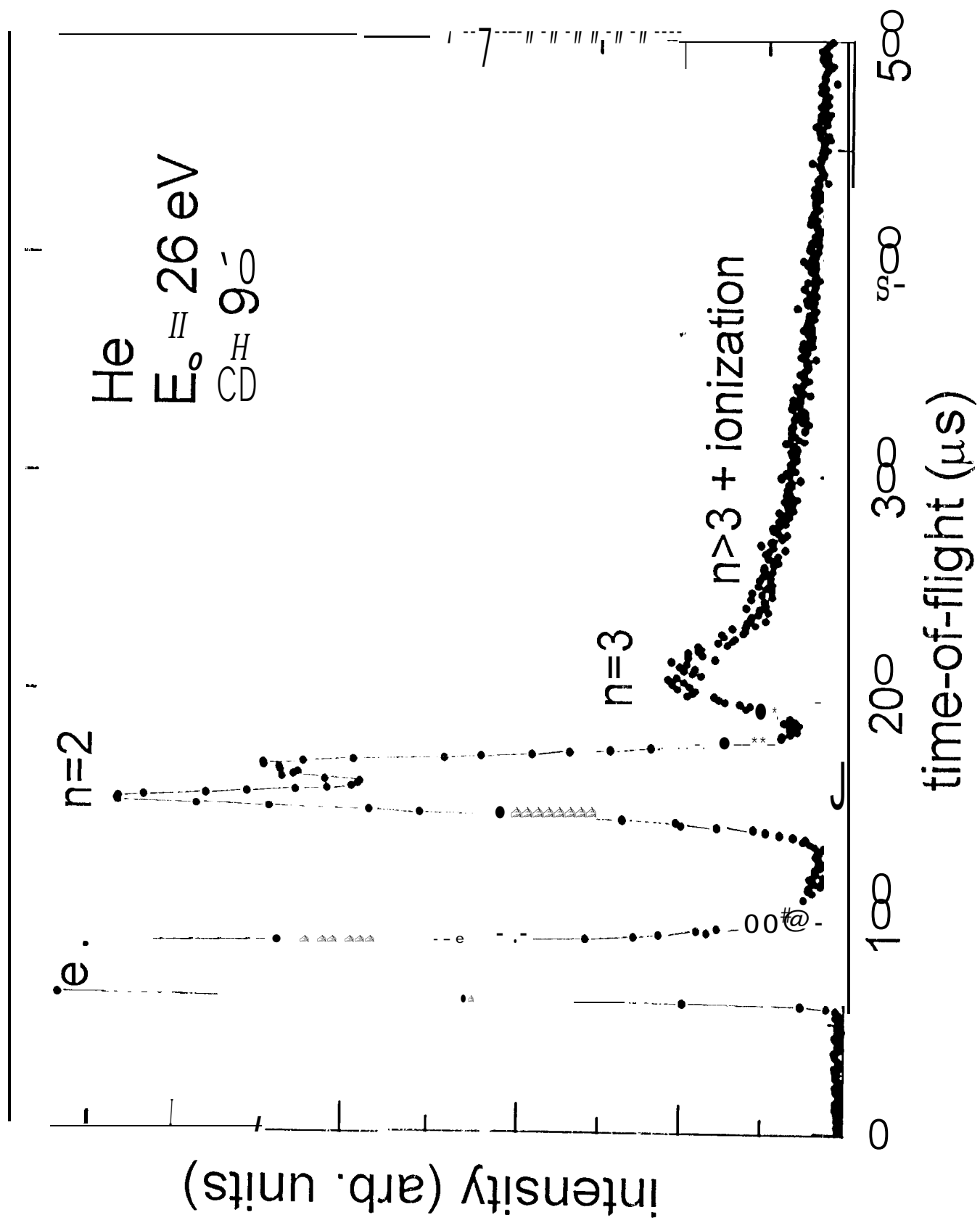
(4) Zetner et al. (1996)

Figure Captions

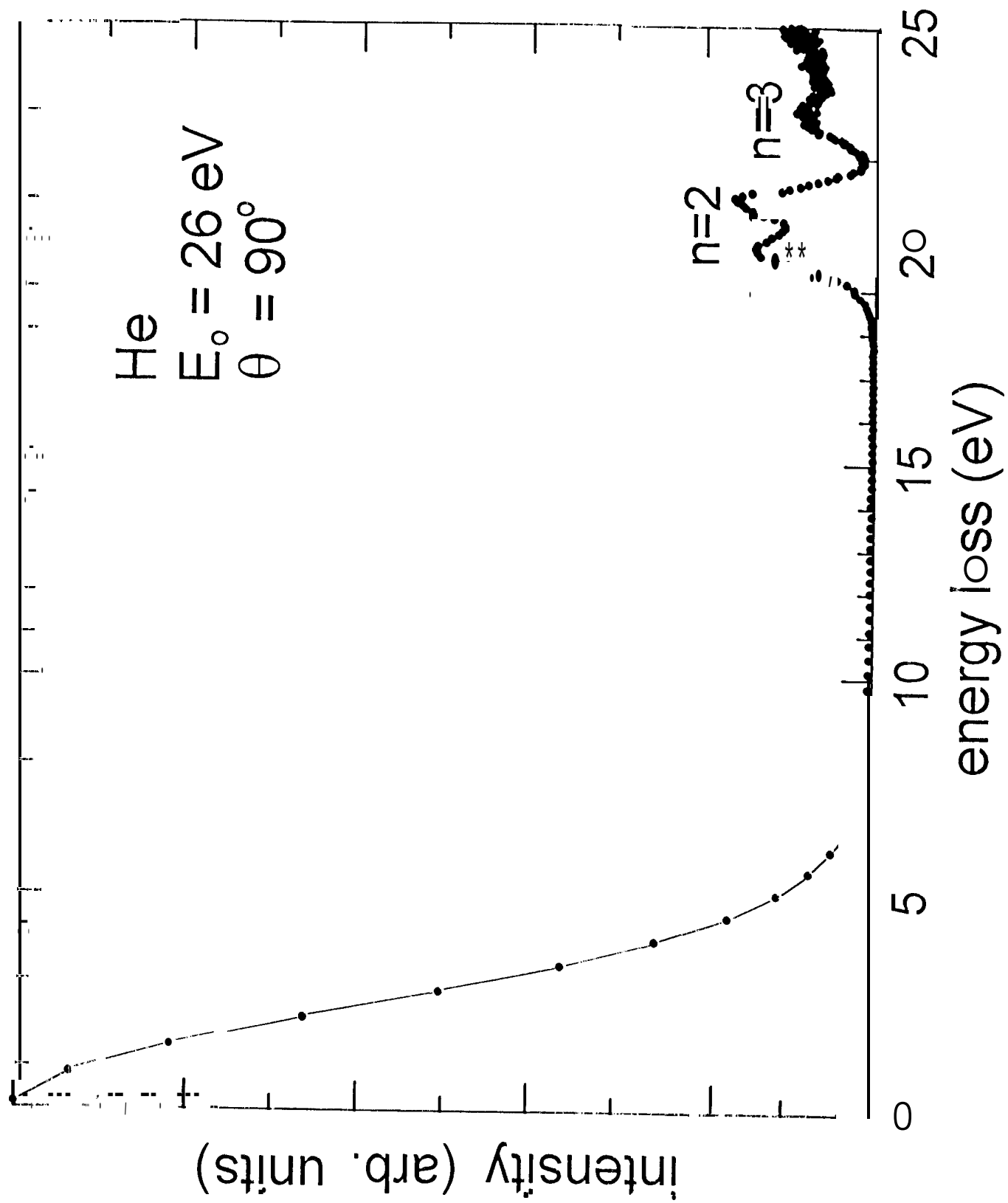
1. (a) Time of flight (TOF) spectrum for electron scattering by 1 Ie at 26 eV impact energy and 90° scattering angle (see text for explanation). (b) The energy loss spectrum corresponding to the TOF spectrum shown in a.
2. Differential cross sections for excitation of the $n = 2$ manifold states in 1 Ie at 90° scattering angle. Experimental results: ●, present; ■, Cartwright et al. (1992) and Trajmar et al. (1992); ♦, Allan (1992); ▲, Ball et al. (1973). Theoretical results: ○, FOMBT, Cartwright et al. (1992) and Trajmar et al. (1992) (The point at 50 eV has been placed at 49 eV for clarity); ▲, Fon et al. (1995); [1, Fursa and Bray (1995). Typical error limits for the present results and for other experimental results are shown.
3. Energy loss spectrum of Xc obtained from a TOF spectrum at $E_0 = 12$ eV and $\theta = 90^\circ$. Designation of energy loss features are indicated as I and II.
4. Differential cross sections for excitation of the two lowest levels in Xc at 90° scattering angle. Experimental results: ●, present TOF; ♦, Jester and Kessler (1994); ■, Filipovic et al. (1988); ▲, Nishimura et al. (1985, 1994). Theoretical results: ○, Khakoo et al. (1996); [1, Bartschat and Madison (1992 a, b and 1995); ▲, Zuo et al. (1991, 1992 a and b). The points at 30 eV for the latter two theoretical results have been placed at 29 eV for clarity. Typical error limits are indicated and some of the data points are connected by arbitrarily drawing solid and dashed lines through the experimental and theoretical data points, respectively.
5. Energy-loss spectra for N₂ at $\theta = 90^\circ$ obtained from TOF spectra. The energy loss region designation is indicated.
6. Inelastic to elastic scattering intensity ratios for regions I, II and III for N₂ at $\theta = 90^\circ$ (given as % of elastic intensity). A few representative error bars are shown.
7. (a) Differential cross section at 90° scattering angle for excitation of the seven electronic states contained in feature I. ●, present TOF; ▲, Brunger and Culmer (1990); +, Cartwright et al. (1977) / Trajmar et al. (1983). Representative error limits are shown. The data points have been connected by arbitrary smooth curves to guide the eye. (b) same as (a) except for region II.
8. Energy-loss spectrum of N₂ at $E_0 = 15.0$ eV, $\theta = 90^\circ$ obtained by a conventional electrostatic spectrometer. The two electronic states and their vibrational structure, for which no overlap from other electronic states occurs, are indicated.
9. (a) Differential cross sections for excitation of the $v = 6$ vibrational level of the $A^3\Sigma_u^+$ electronic state in N₂ at 90° scattering angle. ●, present TOF; ♦, Zobel et al. (1996a) ~ ▼, Brunger and Culmer (1990); ▲, Cartwright et al. (1977) / Trajmar et al. (1983). Representative error limits are shown. The data points have been connected by arbitrary

smooth curves to guide the eye. (b) Same as (a) except for excitation of the combined vibrational levels $v = 4, 5,$ and 6 .

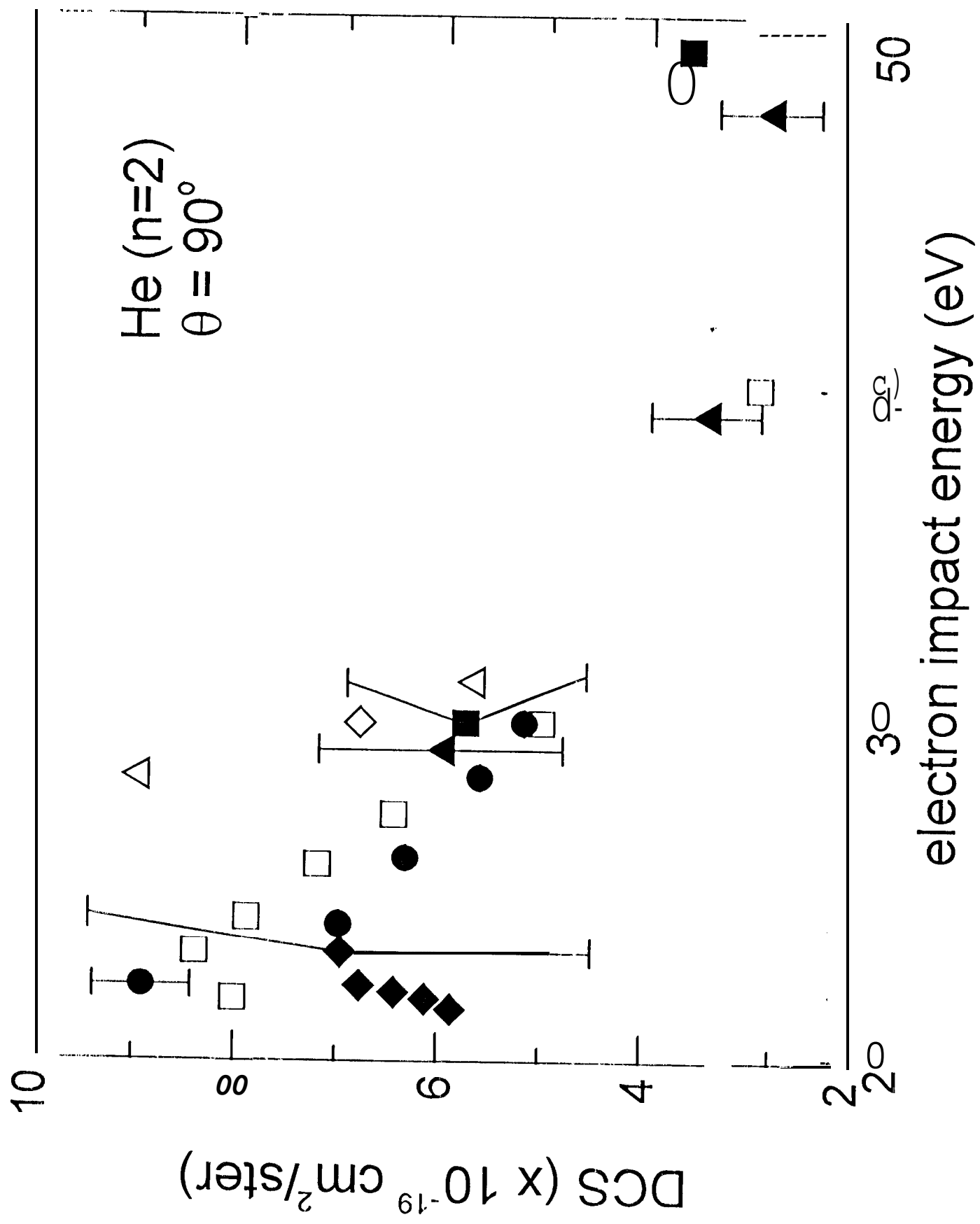
10. Differential cross sections for excitations of the combined $v = 0, 1,$ and 2 vibrational levels in the $C^3\text{11}$, electronic state for CO at $\theta = 90^\circ$. ●, present '1'01"; ♦, Zobel et al. (1996a); ▲, Cartwright et al. (1977)/ Trajmar et al. (1983); ▼, Brunger and Teubner (1990). Representative error limits are indicated. The data points have been connected by arbitrary smooth curves to guide the eye.
11. Energy-loss spectra for CO obtained by the TOF method at $V_0 = 9$ and 13 eV both at $\theta = 90^\circ$. Designations of the energy-loss regions are shown.
12. Differential cross sections for excitation of the $a^3\text{11}$ electronic state in CO at $\theta = 90^\circ$. Experiment: ●, present TOF; ♦, Zobel et al. (1996a); ▲, Middleton et al. (1993). Theory: [1, Sun et al. (1992). Typical error limits are indicated.
13. Differential cross sections for excitation of the $A^1\text{II}$ state and the combined six electronic states contributing to feature 11 in the TOF spectra at $\theta = 90^\circ$ for CO. For $\text{DCS}_{\text{II}}(90)$: ●, present TOF; □, Zetner et al. (1996); ▲, Middleton et al. (1993). For $\text{DCS}_{A^1\text{II}}(90)$: ◇, Zobel et al. (1996b); □, Zetner et al. (1996); ▲, Middleton et al. (1993). The $\text{DCS}_{\text{II}}(90)$ and $\text{DCS}_{A^1\text{II}}(90)$ values are connected by solid and dashed lines, respectively, and typical error bars are shown.



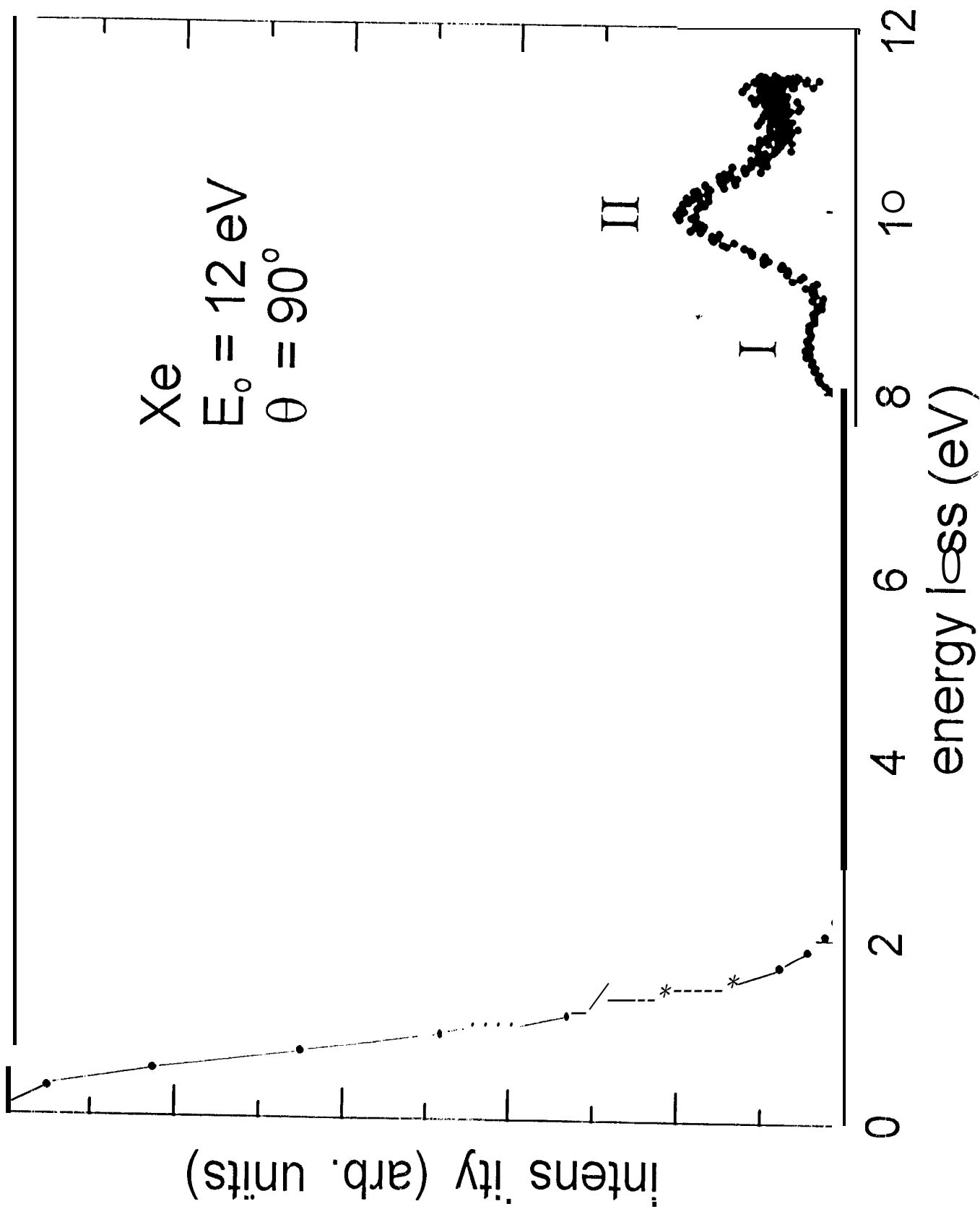
LeClair & Trajmar Fig. 1a



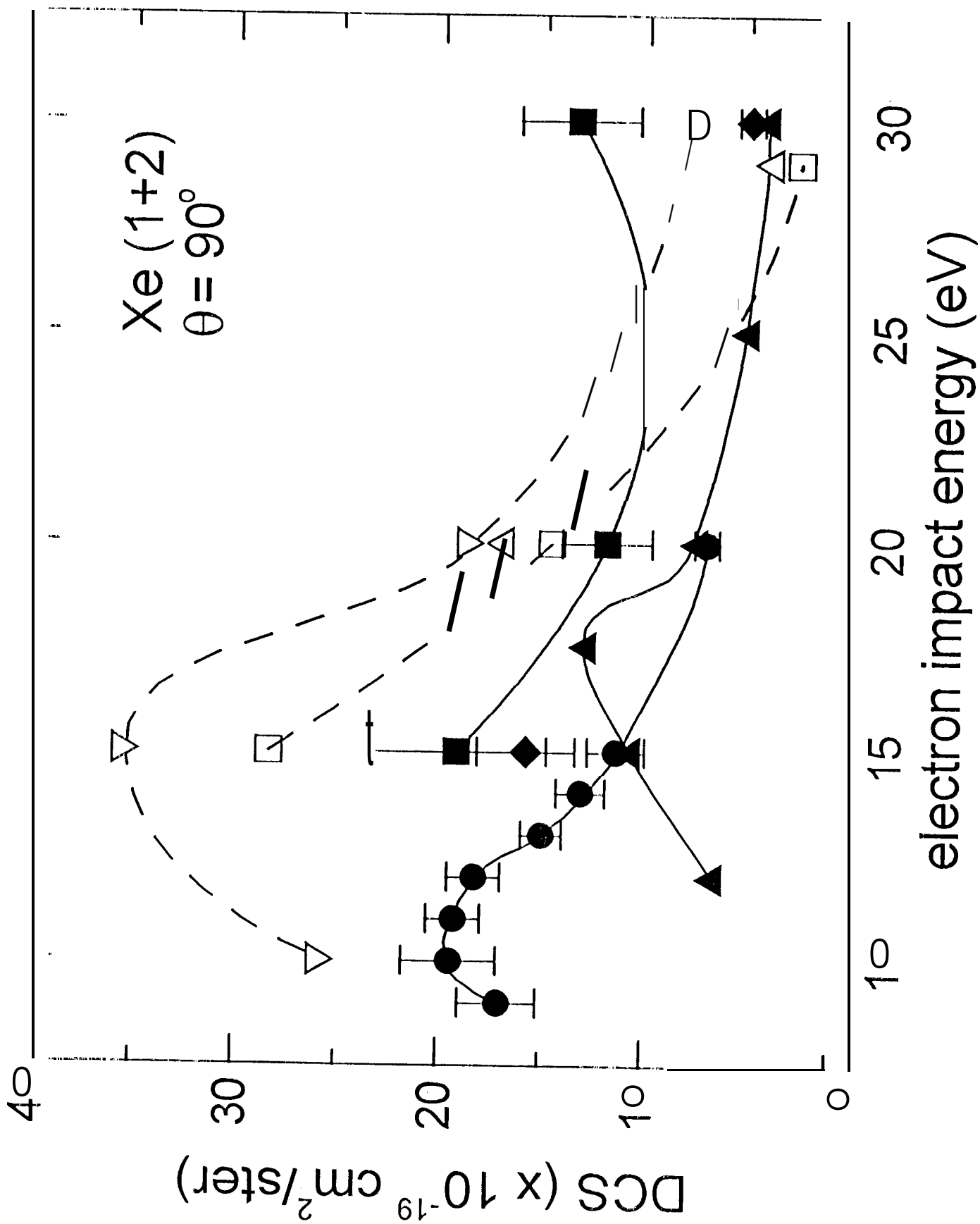
LeClair & Trajmar Fig. 1b



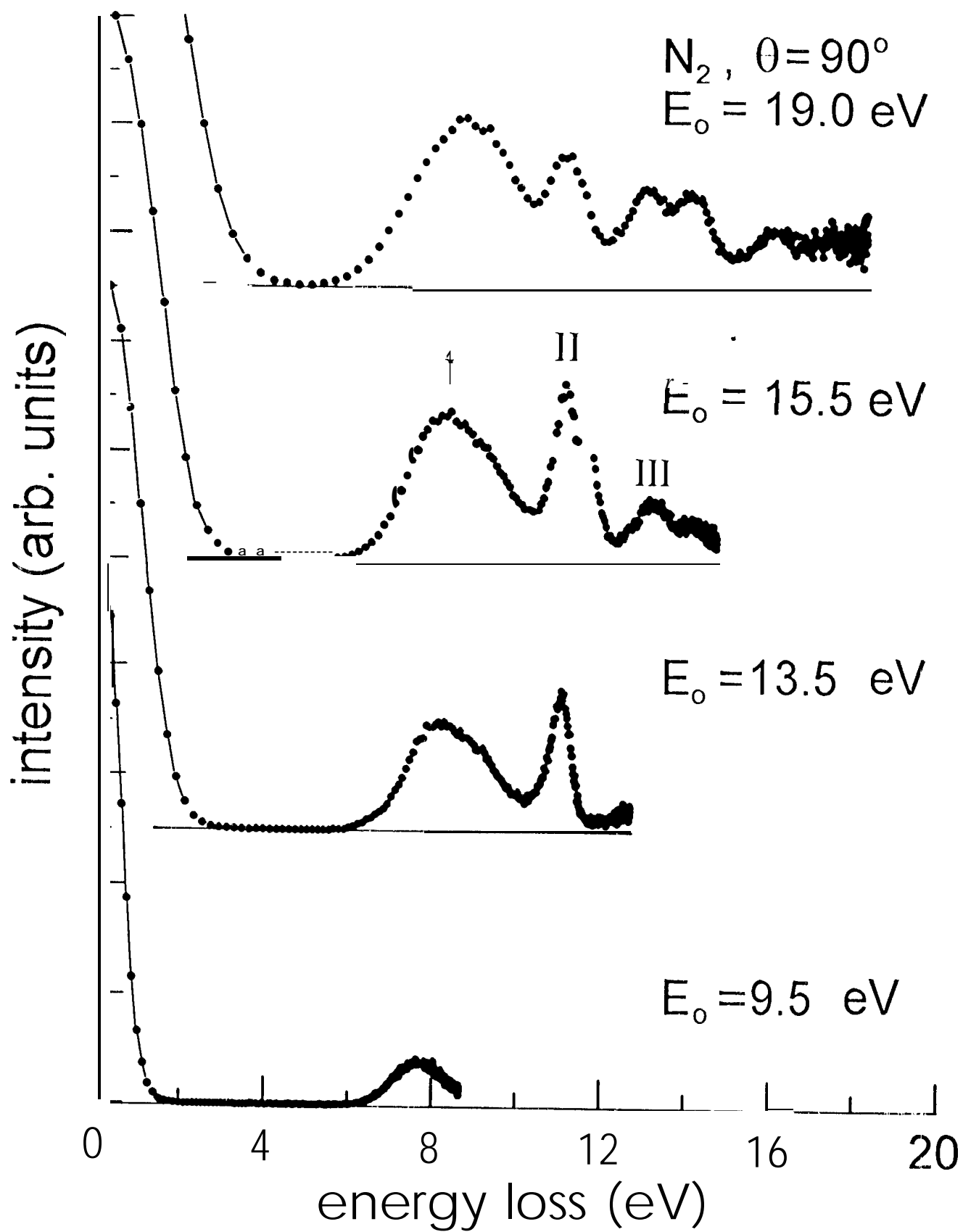
LeClair & Trajmar Fig. 2

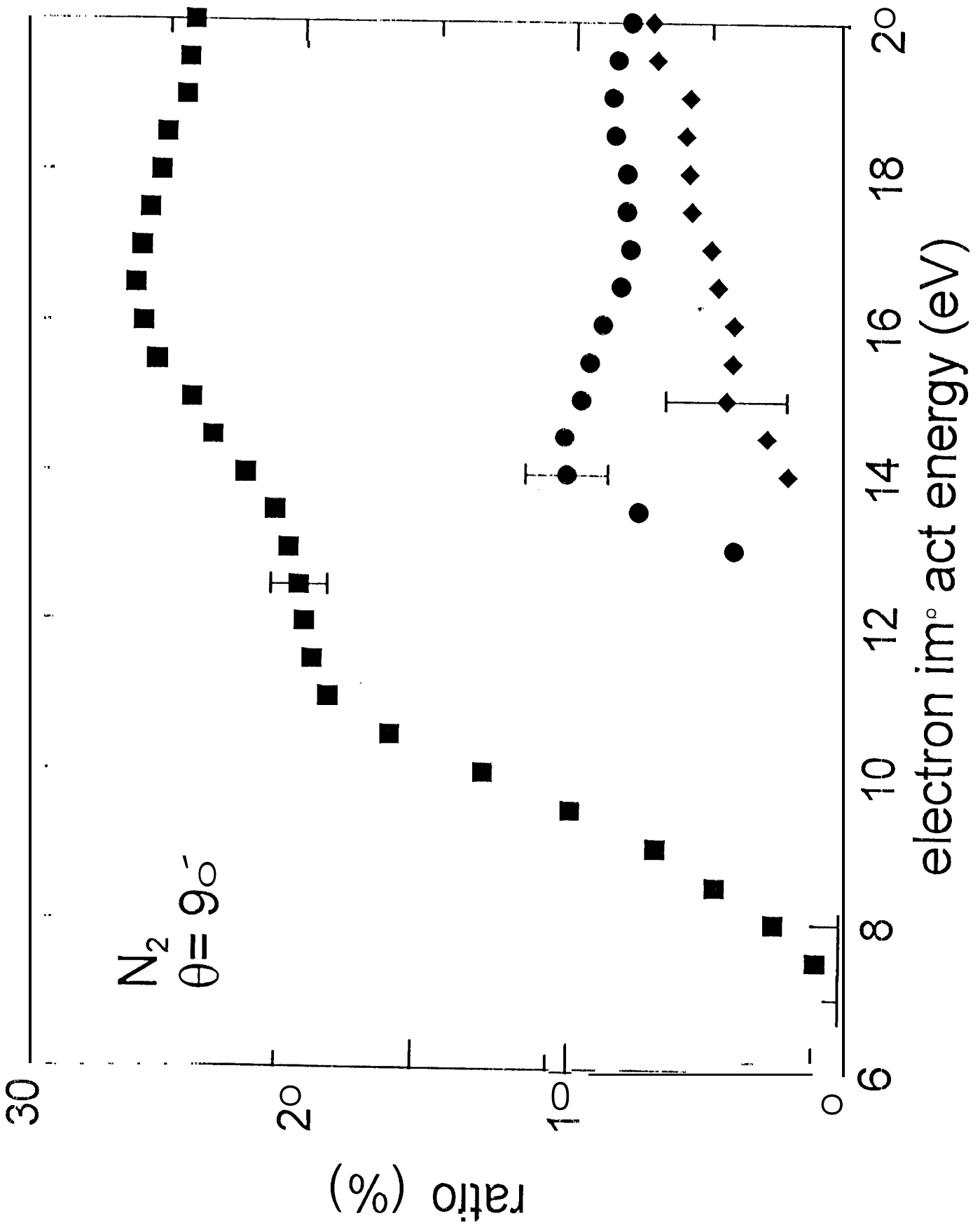


LeClair & Trajmar Fig. 3



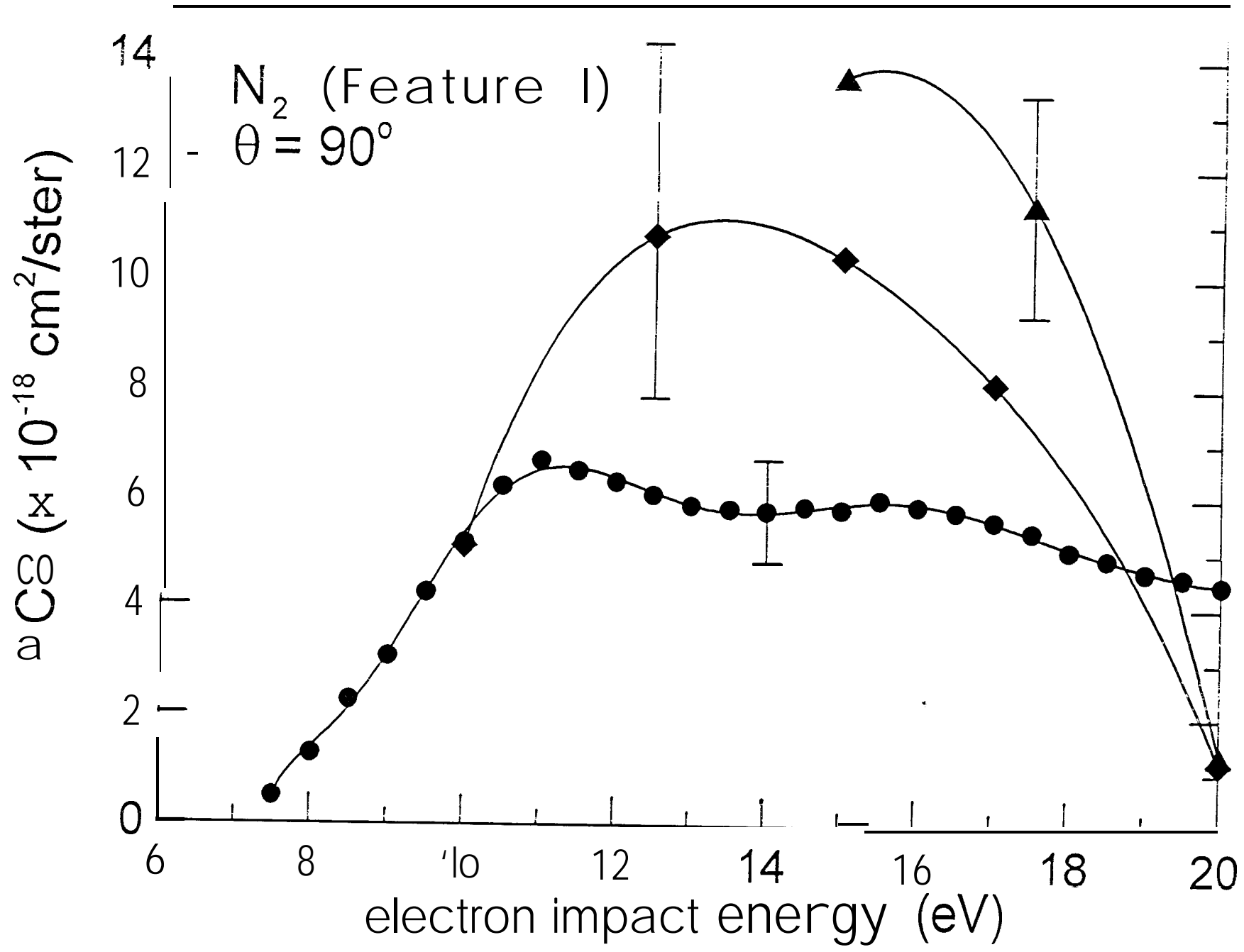
LeClair & Trajmar Fig. 4

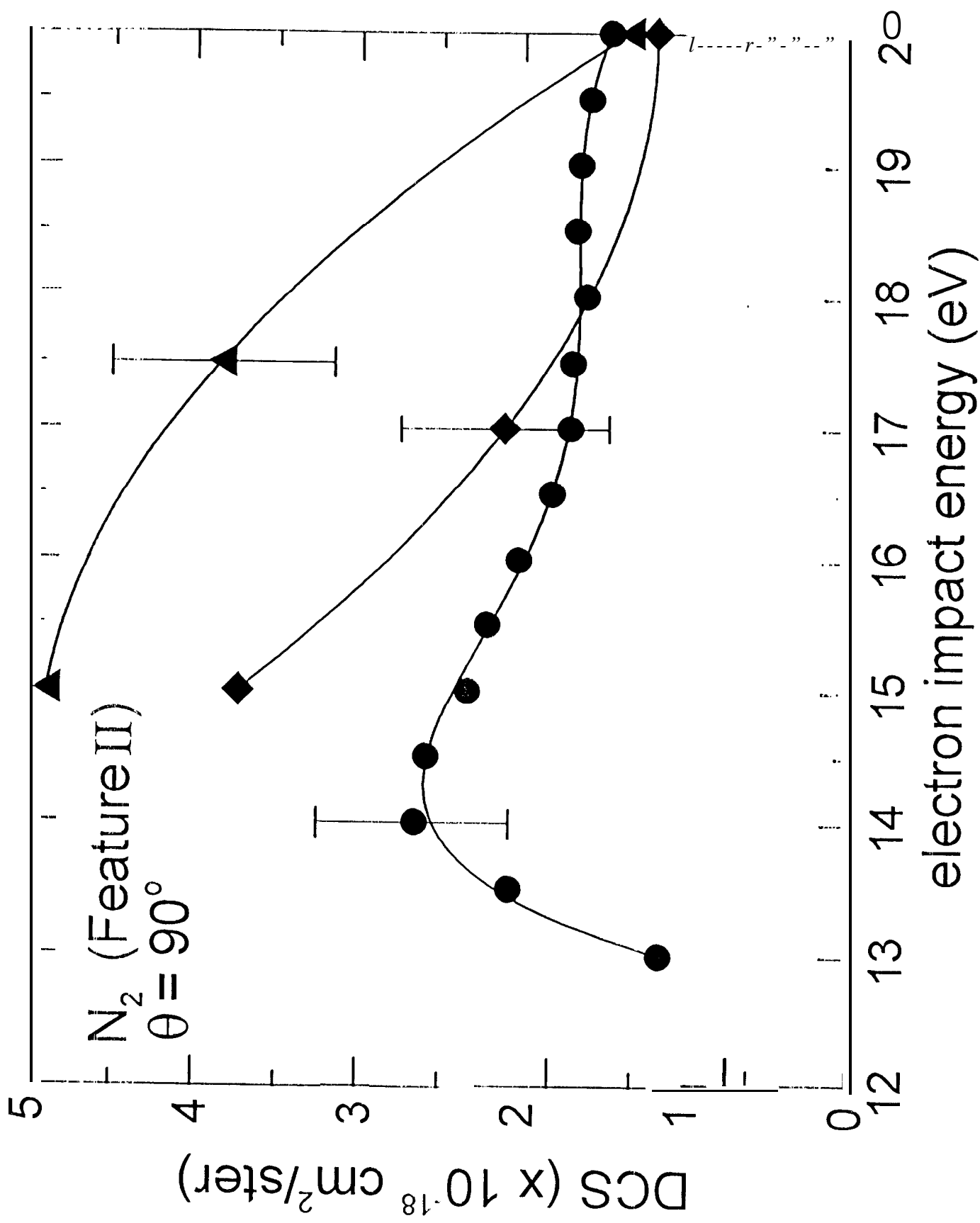




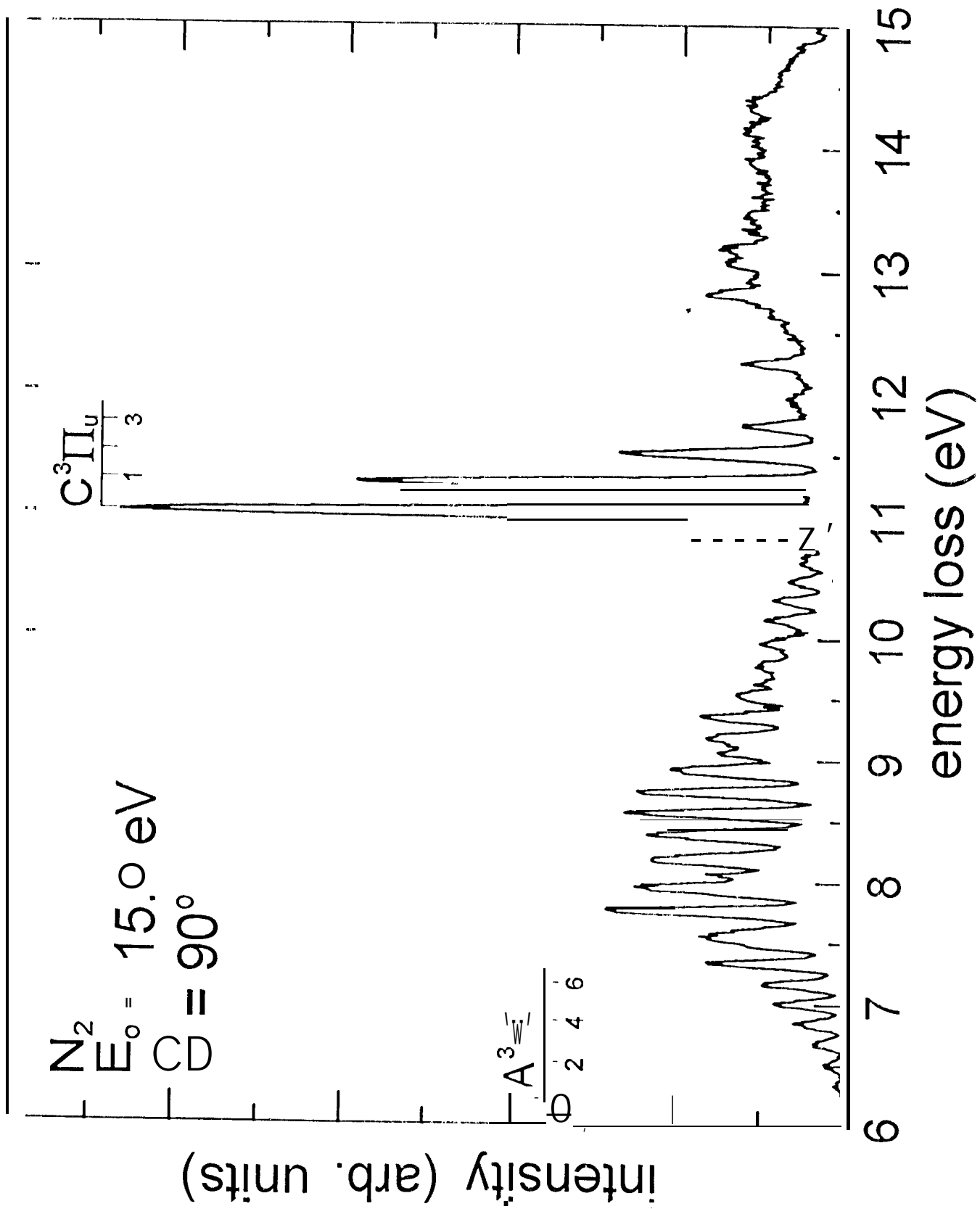
LeClair & Trajmar Fig. 6

Leclair & Trajmar Fig. 7a

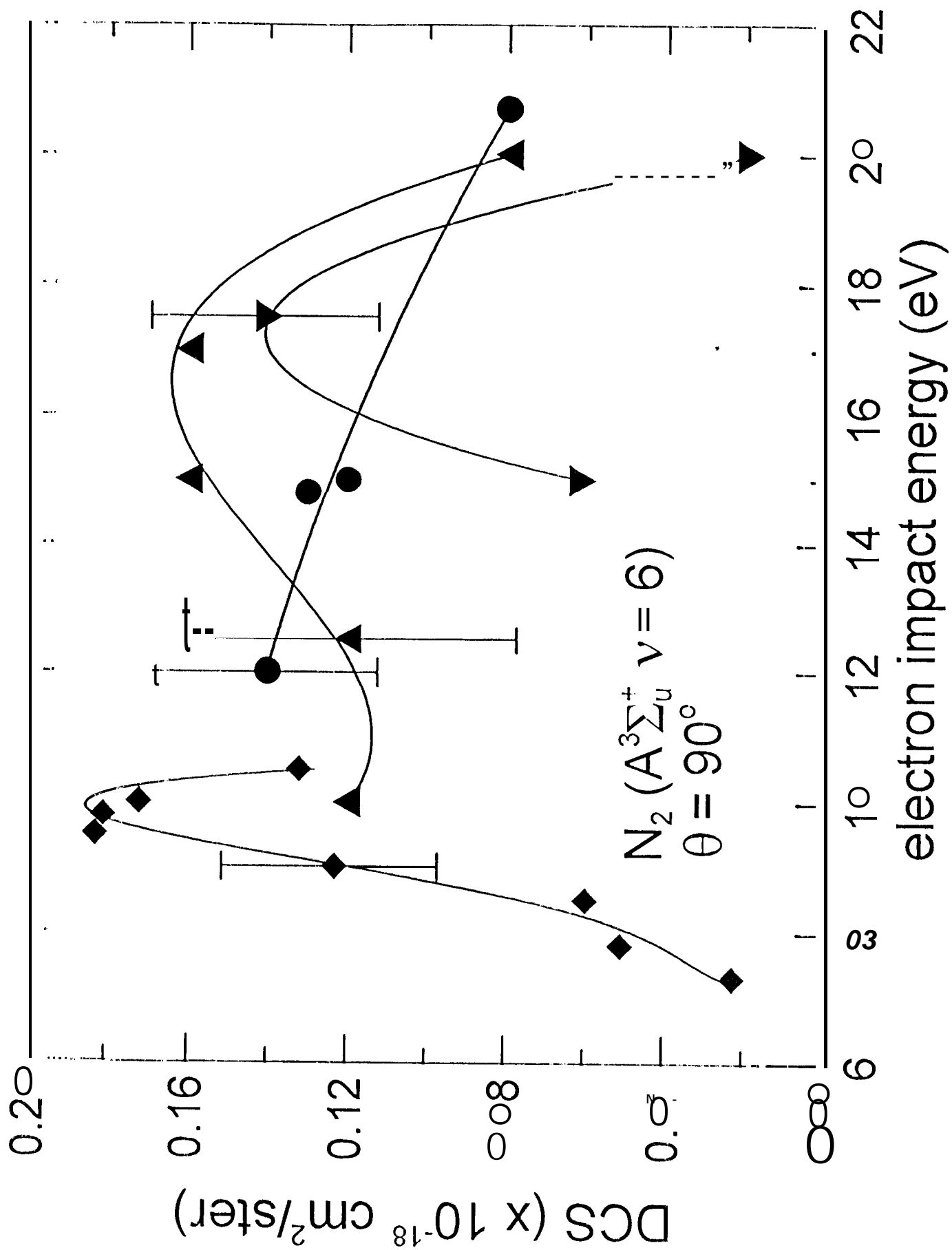




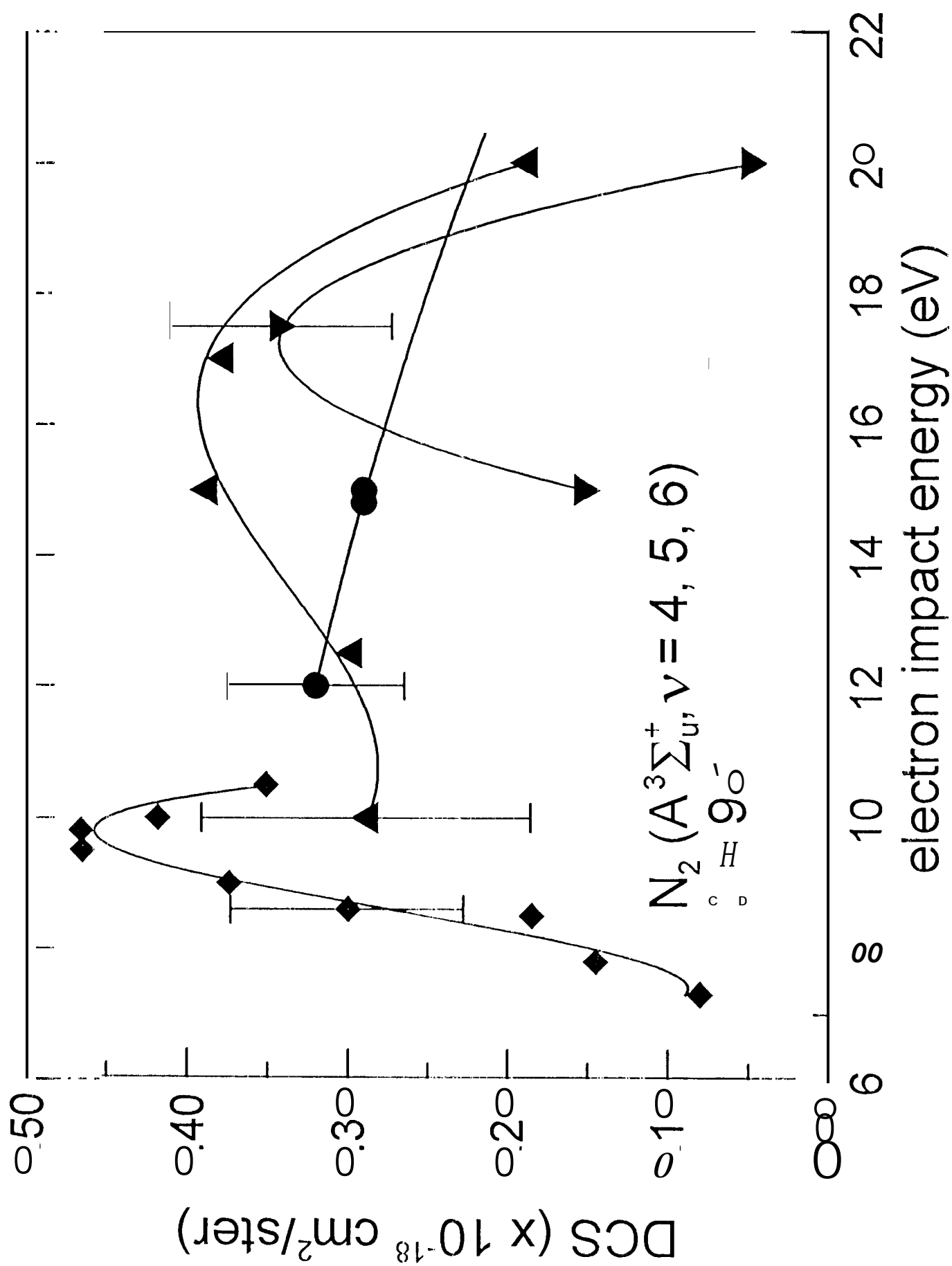
LeClair & Trajmar Fig. 7b



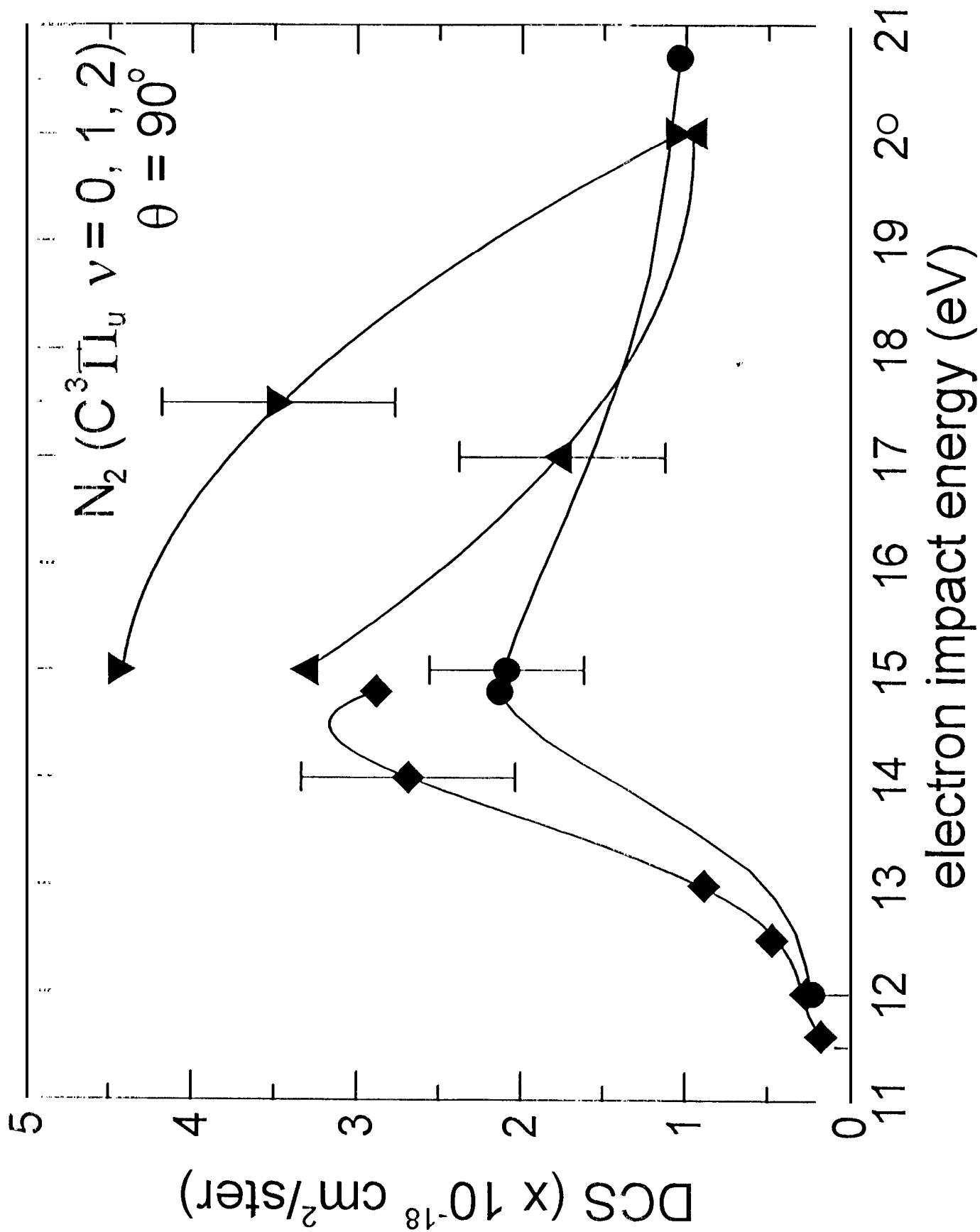
LeClair & Trajmar Fig. 8



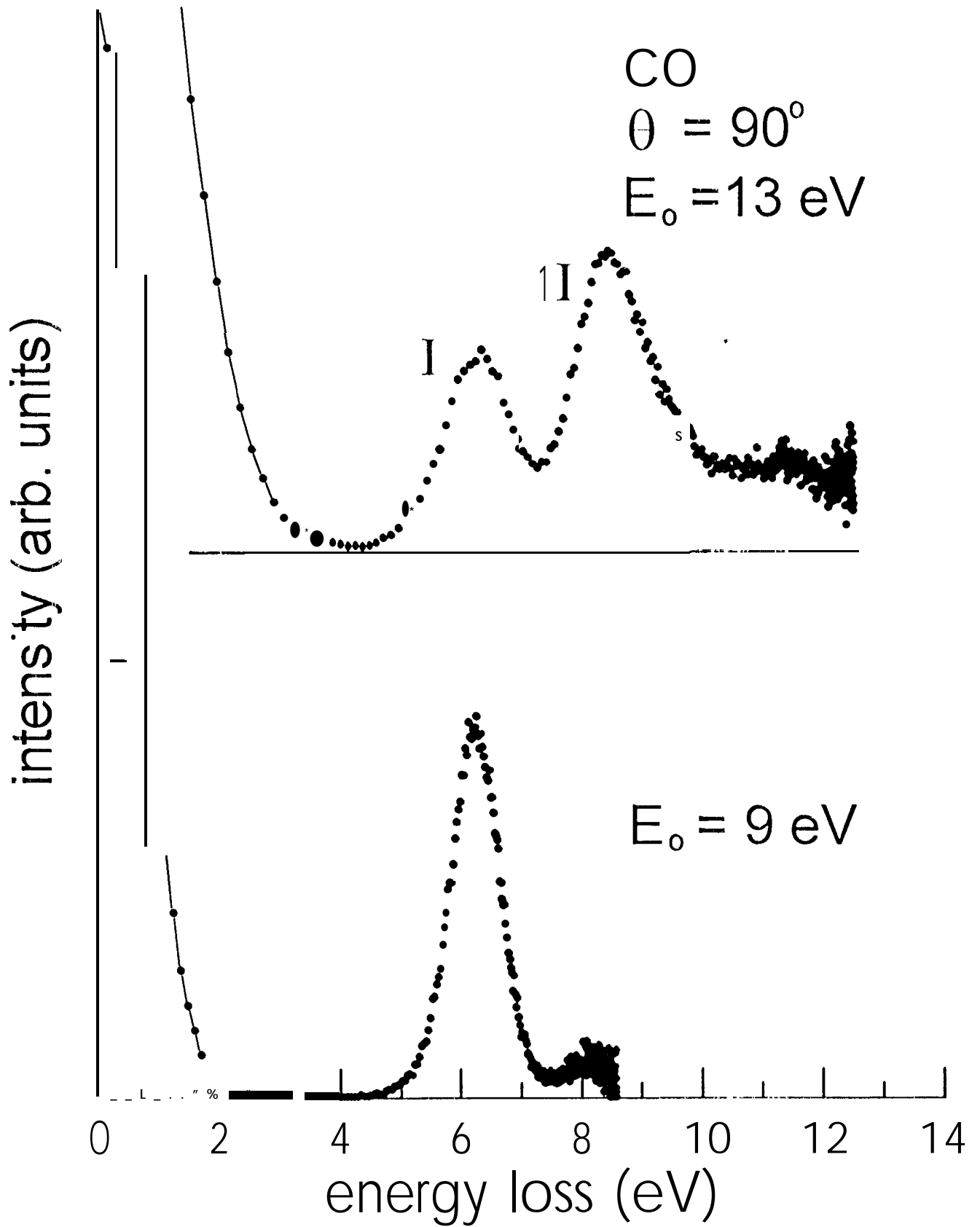
Leclair & Trajmar Fig. 9a

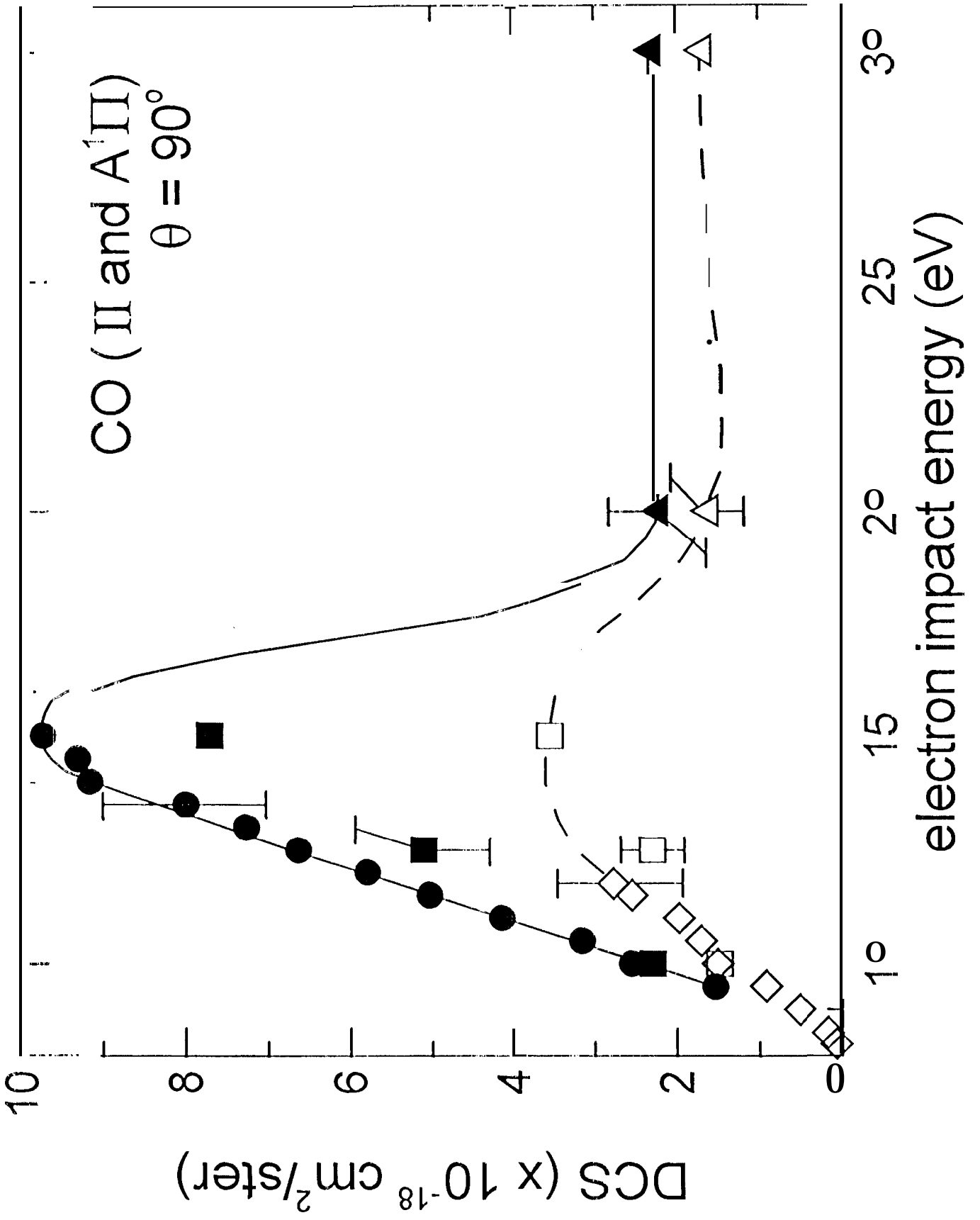


LeClair & Trajmar Fig. 9b



LeClair & Trajmar Fig. 10





Lellair & Trajmar Fig. 13